Mon. Not. R. Astron. Soc. **000**, 1–24 (2013) Printed 22 May 2013 (MN LATEX style file v2.2)

A multi-domain approach to asteroid families identification

V. Carruba[1⋆], R. C. Domingos[2], D. Nesvorný[3], F. Roig[4], M. E. Huaman[1], and D. Souami[5,6]
[1] *UNESP, Univ. Estadual Paulista, Grupo de dinâmica Orbital e Planetologia, Guaratinguetá, SP, 12516-410, Brazil*
[2] *INPE, Instituto Nacional de Pesquisas Espaciais, São José dos Campos, SP, 12227-010, Brazil*
[3] *SWRI, SouthWest Research Institute, 1050 Walnut Street, Suite 300, Boulder, CO 80302, USA*
[4] *ON, Observatório Nacional, Rua General José Cristino 77, Rio de Janeiro, RJ, Brazil*
[5] *UPMC, Université Pierre et Marie Curie, 4 Place Jussieu, 75005, Paris, France*
[6] *SYRTE, Observatoire de Paris, Systèmes de Référence Temps Espace, CNRS/UMR 8630, UPMC, Paris, France;*

Accepted 2013 May 15. Received 2013 May 14; in original form 2013 April 16th.

ABSTRACT

It has been shown that large families are not limited to what found by hierarchical clustering methods (HCM) in the domain of proper elements (a,e,sin(i)), that seems to be biased to find compact, relatively young clusters, but that there exists an extended population of objects with similar taxonomy and geometric albedo, that can extend to much larger regions in proper elements and frequencies domains: the family "halo". Numerical simulations can be used to provide estimates of the age of the family halo, that can then be compared with ages of the family obtained with other methods. Determining a good estimate of the possible orbital extension of a family halo is therefore quite important, if one is interested in determining its age and, possibly, the original ejection velocity field. Previous works have identified families halos by an analysis in proper elements domains, or by using Sloan Digital Sky Survey-Moving Object Catalog data, fourth release (SDSS-MOC4) multi-band photometry to infer the asteroid taxonomy, or by a combination of the two methods. The limited number of asteroids for which geometric albedo was known until recently discouraged in the past the extensive use of this additional parameter, which is however of great importance in identifying an asteroid taxonomy. The new availability of geometric albedo data from the Wide-field Infrared Survey Explorer (WISE) mission for about 100,000 asteroids significantly increased the sample of objects for which such information, with some errors, is now known.

In this work we proposed a new method to identify families halos in a multi-domain space composed by proper elements, SDSS-MOC4 $(a^*, i-z)$ colors, and WISE geometric albedo for the whole main belt (and the Hungaria and Cybele orbital regions). Assuming that most families were created by the breakup of an undifferentiated parent body, they are expected to be homogeneous in colors and albedo. The new method is quite effective in determining objects belonging to a family halo, with low percentages of likely interlopers, and results that are quite consistent in term of taxonomy and geometric albedo of the halo members.

Key words: Minor planets, asteroids: general – Celestial mechanics.

1 INTRODUCTION

Asteroid families are groups of asteroids that are supposed to have a common origin in the collisional event that shattered the parent body. They are usually determined by identifying clusters of objects close in proper elements domain $(a, e, sin(i))$. The Hierarchical Clustering Method (HCM hereafter) as described by Bendjoya and Zappalá (2002) operates by identifying all objects that are closer than a given distance (cutoff) with respect to at least one other member of a family. If an object is closer than this distance, it is associated to the dynamical family, and the procedure is repeated until no new family members are found. The choice of this cutoff distance is then of paramount importance in determining the family. For small values of the cutoff only the objects closest in proper element domain are identified as family members: the family "core". At larger cutoff one is able to identify objects that, while still belonging to the collisional group, may have dynamically evolved since the

⋆ E-mail: vcarruba@feg.unesp.br

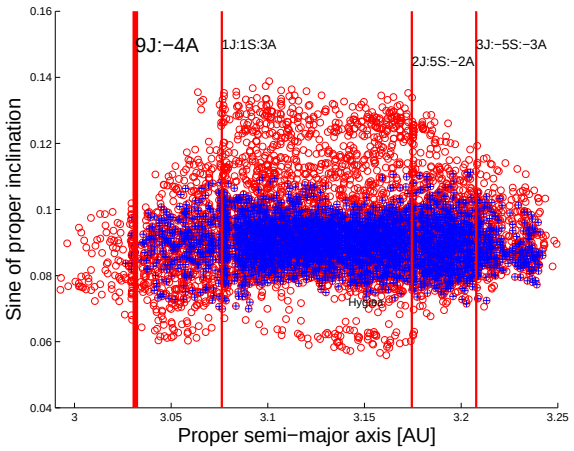

Figure 1. An $(a, sin(i))$ projection of the Hygiea family core (blue crosses) and halo (red circles), as obtained in Carruba (2013). Vertical red lines displays the location of the main mean-motion resonances in the region.

family formation and drifted apart from the core: the family "halo" [1].

To illustrate this issue, Fig. 1 displays the family core (blue crosses) and halo (red circles), as obtained in Carruba (2013) for the Hygiea family, at cutoff of 66 m/s and 76 m/s, respectively. At cutoffs larger than 76 m/s the family merged with other dynamical groups in the region (such as the Veritas and Themis family) and with the local background, thus it was no longer identifiable as a separate entity. Numerical simulations can be used to provide estimates of the age of the family halo, as done, for instance, by Brož and Morbidelli (2013) for the Eos halo, that can then be compared with ages of the family obtained with other methods. Determining a good estimate of the possible orbital extension of a family halo is therefore quite important, if one is interested in determining its age and, possibly, the original ejection velocity field.

One problem in obtaining a good determination of a family halo is however the presence of objects in the orbital region of the halo that might not be connected with the local family. Assuming that most families were created by a breakup of an undifferentiated parent body, we would expect that most of its members should be homogeneous in colors and albedo. Objects that belongs to the dynamical families but that differs in colors or albedo may possibly be asteroids of the local background that just happened to lie in the orbital region of a given family: the interlopers. An analysis of spectral properties of local asteroids may provide insights on the possible presence of such interlopers in groups found in proper elements domains, but such information is usually available only for 2% or less of the main belt asteroids. Yet including too many interlopers into the family may change the perceived orbital structure of the group and cause to obtain distorted estimates of its properties. Recently, the Sloan Digital Sky Survey-Moving Object Catalog data, fourth release (SDSS-MOC4 hereafter, Ivezic et al. 2002), provided multi-band photometry on a sample two order of magnitude larger than any available in any current spectroscopic catalogs (about 60000 numbered objects). While for the purpose of deriving very reliable inferences about asteroid surface compositions, multi-band photometry is not as precise as spectroscopy. Nesvorný et al. (2005) showed that the SDSS-MOC is a useful data-set to study general statistical variations of colors of main belt asteroids. These authors used an automatic algorithm of Principal Component Analysis (PCA) to analyze SDSS photometric data and to sort the objects into different taxonomical classes. In particular, PCA can be used to derive linear combinations of the five SDSS colors (u, g, r, i, z), in order to maximize the separation between a number of different taxonomic classes in SDSS data. Two large separated complexes were found in the PCA first two components: the C/X complex and the S complex, with various subgroups identified inside the main complexes. A problem with this approach was however the large errors that affected colors in the ultraviolet band u, and that propagated into the computation of the principal components. To avoid including the $u-$data, other authors (Ivezić et al. 2002, Parker et al. 2008) constructed a color-code diagram in a $(a^*, i-z)$ plane, where

$$a^* = C_1 * (g-r) + C_2 * (r-i) + C_3, \quad (1)$$

and C_1, C_2, and C_3 are numerical coefficients that depend on the color values and on the number of observations in the given database (Roig and Gil-Hutton 2006), and g, r, i, and z, the other SDSS colors, had an accuracy of about 0.03 magnitudes, higher than the average errors in the $u-$band. As in the plane of (PC_1, PC_2), asteroids divided in the $(a^*, i-z)$ plane into three fairly distinct groups, the C-complex ($a^* < 0$) the S-complex ($a^* > 0,\ i-z > -0.13$) , and the V-type asteroids ($a^* > 0,\ i-z < -0.13$, Parker et al. 2008) [2].

Asteroid taxonomy is however also defined by the geometric albedo p_V (roughly, the ratio of reflected radiation from the surface to incident radiation upon it, at zero phase angle, (i.e., as seen from the light source), and from an idealized flat, fully reflecting, diffusive scattering (Lambertian) disk with the same cross-section). C-type asteroids tend to have lower values of geometric albedo than S-type ones, and Tholen asteroid taxonomy (Tholen 1989) used values of p_V to distinguish classes of asteroids inside the X-complex, such as the M-, E-, and P-types. Until recently, however, only about two thousand asteroids had reliable values of geometric albedos (see Tedesco et al. 2002). Initial results from the Wide-field Infrared Survey Explorer (WISE) (Wright et al. 2010), and the NEOWISE (Mainzer et al. 2011) enhancement to the WISE mission recently allowed to obtain diameters and geometric albedo values for more than 100,000 Main Belt asteroids (Masiero et al. 2011), increasing the sample of objects for which albedo values were known by a factor 50. Masiero et al. (2011) showed that, with some exceptions, such as the Nysa-Polana group, asteroid families typically show a characteristic albedo for all members, and

[1] The term halo was first introduced to describe this population of objects by Nesvorný et al. (2006), and then adopted by other authors such as Parker et al. (2008).

[2] The a^* color is nothing but the first principal component PC_1 of the data distribution in the (g-r) vs (r-i) color-color diagram.

that a strongly bimodal albedo distribution was observed in the inner, middle, and outer portions of the Main Belt.

Previous works, such as Bus and Binzel (2002a,b), Nesvorný et al. (2005), found asteroid families in extended domains of proper elements and SDSS-MOC4 principal components data in order to minimize the number of possible interlopers, but such an analysis was not extended to asteroids' geometrical albedo. Here we take full advantage of the newly available WISE data and we introduce a new hierarchical clustering method (HCM, see Bendjoya and Zappalá (2002) for details of the method in proper elements space) in a multi-domain space composed by asteroids proper elements $(a, e, sin(i))$, SDSS-MOC4 colors $(a^*, i-z)$, and WISE geometric albedo (p_V), to identify halos associated with main belt asteroid families. The great advantage of this approach is that any group identified in these domains will most likely to belong to the same taxonomical group, since its members have to share not only similar values of proper elements, but also of taxonomically related information such as $(a^*, i-z)$, and p_V. A shortcoming of this approach is related to the more limited number of asteroids that have data in the three domains at the same time, when compared with the larger number of objects that have only proper elements and frequencies, only SDSS-MOC4 principal components data, only WISE albedo data, or a dual combination of these three quantities. However, groups determined with this new approach may serve as a first step in determining the real orbital extension of the families cores and halos, with a precision that other methods already in use in the literature may lack.

This work is so divided: in Sect. 2 we discuss the basics of our approach for finding halos in the multi-domain space. In Sect. 3 we compare the efficiency of this approach in finding low numbers of interlopers with the results of other methods used for identifying asteroid families. In Sects. 4, 5, 6 we apply our method to all the currently known major families in the inner, central, and outer main belt. In Sects. 7 and 8 we discuss the case of the asteroids in the Cybele group and in the Hungaria region. Finally, in Sect. 9 we present our conclusions.

2 METHODS

In this work we are trying to make best use of all the new data on surface colors (SDSS-MOC4) and geometric albedo (WISE and NEOWISE) that is currently available to try to find the most possibly accurate determination of all major main belt family halos. For this purpose we determined the main belt asteroids with synthetic proper elements available at the AstDyS site http://hamilton.dm.unipi.it/cgi-bin/astdys/astibo, accessed on January 15^{th}, 2013 (Knežević and Milani 2003) that also have SDSS-MOC4 and WISE albedo data, and errors in proper elements $(a, e, sin(i))$ less than what described as "pathological" in Knežević and Milani (2003), i.e., $\Delta a > 0.01$ AU, $\Delta e > 0.1$, and $\Delta sin(i) > 0.03$. We computed the SDSS-MOC4 colors $(a^*, i-z)$ and theirs errors, computed with standard propagation of uncertainty formulas under the assumption that the SDSS-MOC4 calibrated magnitude behave as uncorrelated variables. For our sample of 58955 asteroids with SDSS colors, we found values of the coefficients C_1, C_2, and C_3 in Eq. 1 of 0.93967, 0.34208 and -0.6324, respectively. To avoid including data affected by too large uncertainties, we eliminated from our sample asteroids with errors in a^* or $(i-z)$ larger than 0.1 magnitudes. As a test of the validity of our approach we also computed PC_1, PC_2 principal components according to the approach of Novakovic et al. (2011), with their errors, and also rejected objects with errors larger than 0.1. While 68.1% of the asteroids in the SDSS-MOC4 sample passed the conversion into $(a^*, i-z)$ colors and the rejection of noisy data, only 42.08% of the same asteroids had errors in PC_1, PC_2 less than 0.1 [3]. Based on these results, we decided to work with $(a^*, i-z)$ colors rather than principal components. We also eliminated from our sample asteroids with errors in p_V larger than 0.05 if $p_V < 0.2$, and asteroids with errors in p_V larger than 0.1 if $p_V > 0.2$. The stringent constraint on errors in geometric albedo p_V for low albedo asteroids was required to better distinguish between CX-complex asteroids ($p_V < 0.1$) and S-complex asteroids ($p_V > 0.1$). Since some objects in the inner main belt and Hungaria region have values of albedo in the WISE survey that are too high (up to 0.8-0.9) and are possibly an artifact of the method used to calculate absolute magnitude (Masiero et al. 2011), we also eliminated all objects in these two regions (essentially those with semi-major axis smaller than that of the center of the 3J:-1A mean-motion resonance, i.e., about 2.5 AU) with $p_V > 0.5$ from our database.

We then defined a distance metrics between two asteroids in a multi-domain space as

$$d_{md} = \sqrt{d^2 + C_{SPV}[(\Delta a^*)^2 + (\Delta(i-z))^2 + (\Delta p_V)^2]}, \quad (2)$$

where, $\Delta a^* = a_2^* - a_1^*$ and similar relations hold for $\Delta(i-z)$ and Δp_V. Following the approach of Bus and Binzel (2002a,b) for a similar distance metric of proper elements and SDSS-MOC principal components (see also Nesvorný et al. 2005, Carruba and Michtchenko 2007), C_{SPV} is a weighting factor equal to 10^6 (other choices in a range between 10^4 to 10^8 have been tested without significantly changing the robustness of the results), and d is the standard distance metrics in proper element domain defined in Zappalá et al. (1995) as:

$$d = na\sqrt{k_1(\frac{\Delta a}{a})^2 + k_2(\Delta e)^2 + k_3(\Delta sin(i))^2}, \quad (3)$$

where n is the asteroid mean motion; Δx the difference in proper a, e, and $sin(i)$; and k_1, k_2, k_3 are weighting factors, defined as $k_1 = 5/4$, $k_2 = 2$, $k_3 = 2$ in Zappalá et al. (1990, 1995). As first halo members, we selected asteroids that belong to the asteroids family, whose spectral type is compatible with that of the other members according to Mothé-Diniz et al. (2005), Nesvorný et al.

[3] The large rejection of noisy data in this later approach is due to the inclusion of the magnitudes in the u filter, which are affected by larger errors that the magnitudes in the other filters. An alternative approach based on principal components PC_1, PC_2 only in g, r, i, and z colors domain was also tried. 67.7% of our data passed the conversion into this space with errors less than 0.1. Since the $(a^*, i-z)$ approach was slightly more efficient and it provided results that are easier to analyze in terms of taxonomies than the principal component approach, in this work we have decided to opt for the $(a^*, i-z)$ method.

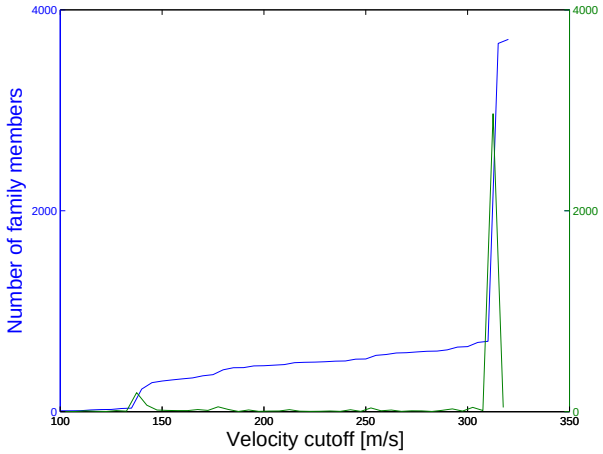

Figure 2. The number of members (blue line) and new members (green line) of the Themis group as a function of the velocity cutoff d_{md}.

(2006), Carruba (2009a,b, 2010b) and other authors, and that, of course, also have acceptable SDSS-MOC4 and WISE/NEOWISE data. For families not treated by these authors, we consulted the list of asteroid families available at the AstDyS site, and the Nesvorný (2012) HCM Asteroid Families V2.0, on the Planetary Data System, available at http://sbn.psi.edu/pds/resource/nesvornyfam.html, accessed on March 13^{th} 2013. We then obtained dynamical groups using Eq. 2, for a value of cutoff d_{md} a bit less than the value for which the family halo merges with the local background (and other families in the region). As an example of this procedure, we choose the case of the Themis family. Fig. 2 displays the total number of members of this group (blue line) and the number of new members of the group (green line, as new members we mean the number of objects that became part of the group at that given velocity cutoff), as a function of the velocity cutoff d_{md}. For $d_{md} = 315$ m/s the Themis halo merged with other local groups, such as the Hygiea family, so we choose in this case to work with a halo defined at $d_{md} = 310$ m/s.

An advantage of the method here proposed is that it should automatically select asteroids close in proper elements, SDSS-MOC4, and WISE albedos, so reducing the number of interlopers usually found in dynamical group encountered in proper elements (or frequencies) domains only. This can be verified by an analysis of the SDSS-MOC4 and WISE albedo data of the group so obtained. Again, for the case of the Themis family, Fig. 3 shows a projection in the $(a^*, i-z)$ plane (panel A) and a histogram of the relative distribution of p_V values (panel B) of members of the Themis halo obtained with this method. The Themis family is made mostly by asteroids with CX-complex taxonomy, that in the $(a^*, i-z)$ plane appear on the left of the vertical dotted line, but 9 asteroids have colors incompatible with such classification and should be considered as interlopers. This is confirmed by an analysis of p_V values, where most of the albedos are below 0.1, the threshold for CX-complex asteroids, but there is a tail of objects with higher albedos. The percentage of possible interlopers found with this method, 1.30%, is indeed quite inferior to the $\simeq 10\%$ statistically expected in dynamical families obtained only in proper elements domains (Migliorini et al. 1995). We will discuss how this new approach fares when compared with other methods already known in the literature in the next section.

3 COMPARISON WITH HCM IN OTHER DOMAINS

A natural question that may arise is why studying families halos in a domain of proper elements, SDSS-MOC4 colors, and WISE albedos. How do the results obtained with this approach compare to those obtained with more traditional methods, such as the HCM in proper elements domain, or in a domain of proper elements and SDSS-MOC a^* and $i-z$ colors? To answer this question we obtained asteroid families halos for several groups with the standard distance metrics in proper element domain d of Zappalá et al. (1995), with a metrics in proper elements and SDSS-MOC4 colors domains, given by:

$$d_{md} = \sqrt{d^2 + C_{SPV}[(\Delta a^*)^2 + (\Delta(i-z))^2]}, \quad (4)$$

where C_{SPV} , as discussed in Sect. 2, is a weighting factor equal to 10^6, and with a newly defined distance metric in proper elements and WISE geometric albedo p_V domain, given by:

$$d_{md} = \sqrt{d^2 + C_{SPV}(\Delta p_V)^2}. \quad (5)$$

We determined families halos with the standard metrics of Zappalá (1995), and Eqs. 4, 5, and 2 for several large families in the main belt . Table 1 summarizes our results for the Hygiea, Koronis, and Eos family halos, where we report the value of the cutoff at which the family was found, the number of halo members, the percentage of SDSS-MOC4 and geometric albedo likely interlopers (see Sect. 2 for a definition of the concept of SDSS-MOC4 and geometric albedo likely interlopers), for the four methods that we used (we will refer to these methods as metrics D, DS, DPV, and $DSPV$). The last column, which reports the sum of the percentage of SDSS-MOC4 and geometric albedo likely interlopers, gives a measure of the efficiency of the method in finding likely interlopers: the lower this index, the better the method is working in avoiding taxonomically uncorrelated asteroids to the family halo. Among the several large families halos that we analyzed, we choose to display the results for the Hygiea, Koronis, and Eos groups because these are families for which the new multi-domain method showed one of the best, medium, and worse results in term of not finding interlopers when compared with the other methods, respectively.

The Hygiea family case was the one for which the new method had the best results among the families analyzed, with an overall efficiency of only 9.86%. In the case of the Koronis family the efficiency was lower (23.00%), but the new method still provided the best results when compared with other approaches. The Eos family was a very peculiar case: most of the family members are K-type, an S-complex type whose a^* values are very close to zero, the limiting value separating CX-complex asteroids and S-complex ones The family is surrounded by CX-complex asteroids, and an analysis only based on distance metric inevitably recognizes as family members many background objects not necessarily connected to the family. Only in the case of this family, we found an efficiency of the new method slightly inferior

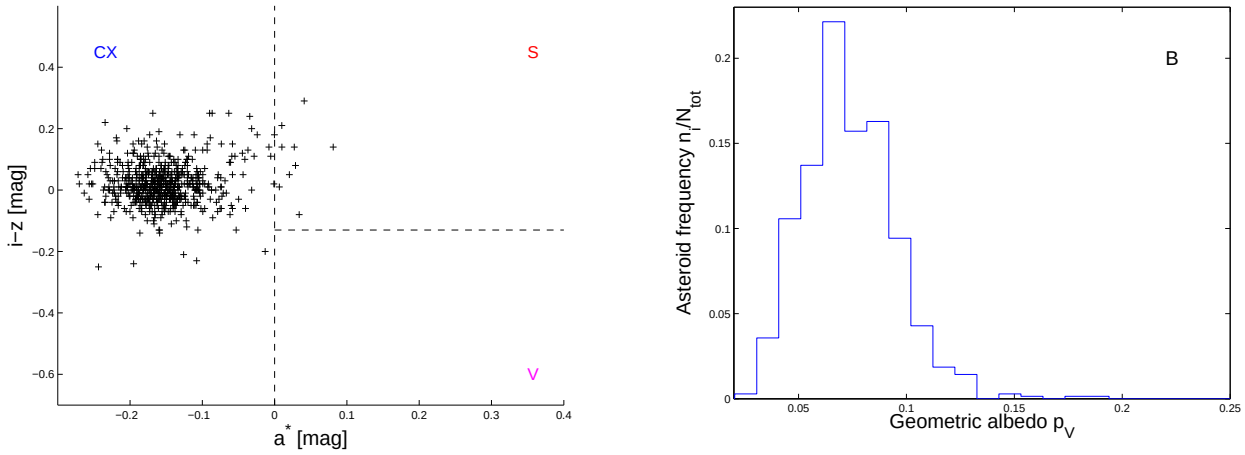

Figure 3. An $(a^*, i-z)$ projection (panel A), and a histogram of the relative distribution of p_V values (panel B) of members of the Themis halo.

Table 1. Efficiency of distance metrics in several domains in finding asteroid families halo members.

Family Name	d_{md} cutoff value $[m/s]$	Number of members	Percentage of SDSS-MOC4 likely interlopers	Percentage of p_V likely interlopers	Metric efficiency
Hygiea halo					
Metric D	80	6152	7.58	15.59	23.17
Metric DS	225	728	5.63	14.02	19.65
Metric DPV	140	2977	8.63	6.45	15.08
Metric $DSPV$	290	426	1.41	8.45	9.86
Koronis halo					
Metric D	65	6958	15.71	14.36	30.07
Metric DS	230	1054	13.54	13.11	26.65
Metric DPV	80	1366	14.32	21.74	36.06
Metric $DSPV$	215	200	16.00	7.00	23.00
Eos halo					
Metric D	40	5322	52.70	17.35	70.05
Metric DS	135	1886	55.99	11.08	67.07
Metric DPV	80	846	57.01	18.94	75.95
Metric $DSPV$	165	738	51.36	17.89	69.25

to the results of the DS metric (69.25% with respect to 67.07%). Overall, the new approach was at its best a factor of two more efficient in eliminating interlopers than other methods, and at its worse provided comparable results to what obtained in the domain of proper elements and SLOAN colors.

Having concluded that the method described by Eq. 2 is the most efficient in term of low numbers of interlopers, we are now ready to start our analysis of the main belt. We will do this by investigating asteroids family halos in the inner main belt.

4 INNER MAIN BELT

The inner main belt is dynamically limited in semi-major axis by the 3J:-1A mean-motion resonance at high a (Zappalá et al. 1995). The 7J:-2A mean-motion resonance is sometimes used by some authors as the boundary between

the inner main belt at high inclination and the region of the Hungaria asteroids. In this work we will just use the upper limit in a given by the 3J:-1A mean-motion resonance. The linear secular resonance ν_6 separates the low-inclined asteroid region from the highly inclined area, dominated by the Phocaea family (see Carruba 2009b, 2010a for a discussion of the local families groups and dynamics). The Phocaea family is located in a stable island limited by the 7J:-2A and 3J:-1A in semi-major axis, and by the ν_6 and ν_5 secular resonances in inclination (Knežević and Milani 2003). We found 2366 objects that have proper elements and frequencies, SDSS-MOC $(a^*, i-z)$ colors, WISE geometric albedo data in the inner main belt, and reasonable errors, according to the criteria defined in Sect. 2. We will start our analysis by studying the case of the Belgica family.

4.1 The Belgica family

The Belgica group was a clump associated with the former Flora family and identified by Mothé-Diniz et al. (2005) as a small and sparse group of only 41 members at a cutoff in proper element domain of 57.5 m/s. Here we found that the halo of the Belgica family merges with that of the Baptistina group already at a cutoff of 100 m/s. We will therefore treat the Belgica family together with the Baptistina cluster.

4.2 The Baptistina family

The Baptistina family, as the Belgica group, was studied by Mothé-Diniz et al. (2005) and was part of the former Flora family. It is located in a very complex dynamical region (Michtchenko et al. 2010), being crossed by powerful mean-motion resonances such as the 7J:-2A and interacting with secular resonances such as the $z_2 = 2(g-g_6)+(s-s_6)$. It has been obtained in the (n, g, s) frequency domain by Carruba and Michtchenko (2009) to study possible diffusion of its members in $s-$type resonances such as the $\nu_{17}+\nu_4+\nu_5-2\nu_6$. Here we identified a 56 members CX halo at a cutoff of 250 m/s. The taxonomical structure of the halo is indeed very complex and puzzling. The majority of the Baptistina halo members have SDSS-MOC4 data compatible with a CX-complex taxonomy, with only 2 members (3.6% of the total) that are possible interlopers. The albedo data is however very puzzling, since 47 members (83.9% of the total) have values of $p_V > 0.1$, not usually associated with dark CX-complex asteroids. Baptistina family members seem to behave as the members of the Hungaria group, a CX-complex family, characterized by large values of albedos (see Sect. 8.1). Understanding the properties of the Baptistina halo will require a much more in depth analysis than what we performed in this work.

4.3 The Vesta family

The Vesta family is unique in the main belt, since it is made mostly by V-type asteroids, that are associated with a basaltic composition, typical of differentiated objects with a crust. Of the many possible differentiated or partially differentiated asteroids that may have existed in the primordial main belt, (4) Vesta is the largest remnant for which a basaltic crust is still present and was observed by a space mission (Russel et al. 2012). Many V-type objects are observed outside the limits of the traditional HCM family (Carruba et al. 2005, Nesvorný et al. 2008), making this family a test-bed for the application of methods on halo determinations.

We determined a 161 members halo at a cutoff of $d_{md} = 275$ m/s. 46 halo members (28.6% of the total, a considerable fraction of the halo) are possible SDSS-MOC4 interlopers, and 26 asteroids (16.2% of the total) are possible albedo interlopers. Among the asteroids with $a^* > 0$, 58.6% are in a region of the $(a^*, i-z)$ plane associated with V-type objects, according to the criteria defined in Sect. 1, and can be considered as possible V-type candidates.

How efficient is the new method in identifying V-type asteroids outside the Vesta family as members of the halo? Among the V-type asteroids not connected to the traditional HCM Vesta family listed in Carruba et al. (2005), only four objects are present in our multi-domain catalog: (3849), (3869), (4188), and (4434). Of these, two (50% of the total), (3869) and (4188), were part of the Vesta halo as found by our method. Having such a limited sample of objects in our catalog and in the halo, we are not able to achieve any conclusions on the validity of the method for the Vesta halo. The Sidwell, Somekawa, Henninghaack, and Ausonia AstDyS family merge with the Vesta halo at a cutoff of less than 320 m/s.

4.4 The Erigone family

The Erigone family was identified by Nesvorný et al. (2006) as a CX-complex group at a cutoff of 80 m/s. Their analysis appears to be confirmed by this work: we found a 57 member CX-complex group at a cutoff d_{md} of 400 m/s. No SDSS-MOC4 interlopers were found in the halo, and only one object (1.8% of the total) was (barely) a possible albedo interloper. The Maartes AstDyS family merges with the Erigone halo at a cutoff of $d_{md} = 165$ m/s.

4.5 The Massalia family

The Massalia family was identified by Nesvorný et al. (2006) as an S-complex family at a cutoff of 50 m/s. In this work we identified 19 S-complex members at a cutoff d_{md} of 250 m/s. Seven SDSS-MOC4 interlopers (36.8% of the total) were found in the halo, and 10 objects (52.6% of the total) were possible albedo interlopers. Incidentally, (20) Massalia itself is a C-type asteroid, and quite likely an interloper in its own family.

4.6 The Nysa/Mildred/Polana family

The Nysa/Polana family was studied by Mothé-Diniz et al. (2005) that confirmed previous results about the dual structure of the family, made by an S-type member group around (878) Mildred, and an F-type group around (142) Polana. In this work we find a CX-complex halo of 147 members at a cutoff d_{md} of 280 m/s. The halo is dominated by the CX-complex Polana group, that is also made by the largest bodies in the area (Mothé-Diniz et al. 2005): we found no possible SDSS-MOC4 interlopers, and 1 (0.7% of the total)

albedo interloper. A smaller halo associated with the Mildred family merges with the larger Polana halo at about 150 m/s, and the Clarissa Planetary Data System is englobed at a cutoff of 345 m/s.

4.7 The Euterpe family

The Euterpe family is a low-inclination group listed by the Planetary Data System. In this work we identified an S-complex halo at a cutoff d_{md} of 335 m/s. Two objects (22.2% of the total) were possible SDSS-MOC4 interlopers, and one asteroid (11.1% of the total) is a possible albedo interloper.

4.8 The Lucienne family

The Lucienne family is a relatively high-inclination group listed by the Planetary Data System. Unfortunately we could not find any member of this group in our multi-domain sample of asteroids for the inner main belt, so no conclusions are possible to achieve on this cluster.

4.9 The Phocaea family

The Phocaea family has been studied by Knežević and Milani (2003) and by Carruba (2009b). It is located in a stable island bounded by the ν_6 and ν_5 secular resonances in inclination and the 7J:-2A and 3J:-1A mean-motion resonances in semi-major axis. Despite the peculiar dynamical configuration, Carruba (2009b) concluded that it was likely that the Phocaea family was a real S-complex collisional family, with an estimated age of about 2.2 Byr. In this work we found an 80 members S-complex halo at a cutoff $d_{md} > 800$ m/s, which is the value for which all asteroids in the stable island in our database were found connected to the Phocaea family. 27 objects (33.8% of the total) were possible SDSS-MOC4 interlopers, and 16 asteroids (20.0% of the total) had values of $p_V < 0.1$. Overall, we confirm the analysis of Carruba (2009b) on the possible reality of the Phocaea family as an S-complex collisional group.

4.10 The inner main belt: an overview

Our results for the inner main belt are summarized in Table 2, where we give information on the first halo member used to determine the family halo, the cutoff value used to identify the halo, the number of bodies in the halo, the spectral complex to which the majority of halo members belongs, and the number of possible interlopers, according to SDSS-MOC4 and geometric albedo considerations.

Fig. 4, panel A, displays an $(a, sin(i))$ projection of asteroids in our multi-variate sample in the central main belt. Vertical red lines identify the orbital position of the main mean-motion resonances in the area. Blue lines show the location of the main linear secular resonances, using the second order and fourth-degree secular perturbation theory of Milani and Knežević (1994) to compute the proper frequencies g and s for the grid of (a, e) and $(a, \sin(i))$ values shown in Fig. 4, panel A, and the values of angles Ω, ω, M, and eccentricity of (25) Phocaea, the highly inclined asteroid associated with the largest family in the region (Carruba 2009b). The orbital position in the $(a, \sin(i))$ plane of the first numbered asteroid in all the inner main belt groups is also identified in Fig. 4, panel A. In panel B of the same figure we display a density map of the inner main belt, according to the approach described in Carruba and Michtchenko (2009). Density maps display regions characterized by strong mean-motion or secular resonances by a relatively low number of asteroids per unit bin. To quantitatively determine the local density of asteroids, we computed the log_{10} of the number of all asteroids with proper elements per unit square in a 22 by 67 grid in a (starting at $a = 2.18$ AU, with a step of 0.015 AU) and $sin(i)$ (starting at 0, with a step of 0.015). Superimposed to the density map, we also show the orbital projection of the halos found in this work shown as plus signs for CX-complex families, and circles for S-complex families. The other symbols are the same as in Fig. 4, panel A.

Fig. 5 displays a projection in the $(a^*, i - z)$ plane of all asteroids in our multi-domain sample (panel A), and an $(a, sin(i))$ projection of the same asteroids, (panel B), where objects in the CX complex are shown as blue circles, and asteroids in the S-complex are identified as red plus signs. The inner main belt is slightly dominated by S-complex asteroids, but with a significant minority of CX-complex bodies. V-type asteroids are mostly concentrated in the Vesta family, but with a significant population outside the dynamical group (see also Carruba et al. 2005).

This is confirmed by an analysis of WISE p_V geometrical albedo data, a histogram of which is presented in Fig. 6, panel A. Fig. 6, panel B, displays an $(a, sin(i))$ projection of the same asteroids, where blue full dots are associated with asteroids with $p_V < 0.1$, red full dots display asteroids with $0.1 < p_V < 0.3$, and magenta full dots show asteroids with $p_V > 0.3$. The majority of asteroids in the inner main belt is made by high albedo objects, associated with S-complex taxonomies, but with a significant minority of CX-complex bodies.

5 CENTRAL MAIN BELT

The central main belt is dynamically limited in semi-major axis by the 3J:-1A and 5J;-2A mean-motion resonances (Zappalá et al. 1995). The linear secular resonance ν_6 separates the low-inclined asteroid region from the highly inclined area, dominated by the Hansa and Pallas families (Carruba 2010b). As discussed in Carruba (2010b), in the highly inclined region the local web of linear secular resonances and mean-motion resonances divided the region into six separated stable islands, each hosting one or more major families, and that can be considered as a stable archipelago. Of particular interest in this region is the Tina family, whose members are all in anti-aligned states of the ν_6 linear secular resonance (Carruba and Morbidelli 2011). We found 3693 objects that have proper elements and frequencies, SDSS-MOC4 a^* and $i - z$ colors, WISE geometric albedo data, and satisfy our error analysis criteria, in the central main belt, and we will start our analysis by studying the case of the Hestia family.

Table 2. Asteroid families halos in the inner main belt.

First halo member	d_{md} cutoff value $[m/s]$	Number of members	Spectral Complex	Number of SDSS-MOC4 likely interlopers	Number of p_V likely interlopers
(298) Baptistina: (4691)	250	56	CX	2	47
(4) Vesta: (2011)	275	161	S(V)	46	26
(163) Erigone: (9566)	400	57	CX	0	1
(20) Massalia: (10102)	250	19	S	7	10
(44) Nysa/Mildred/Polana: (1768)	280	147	CX	0	1
(27) Euterpe: (5444)	335	9	S	2	1
(25) Phocaea: (3322)	> 800	80	S	27	16

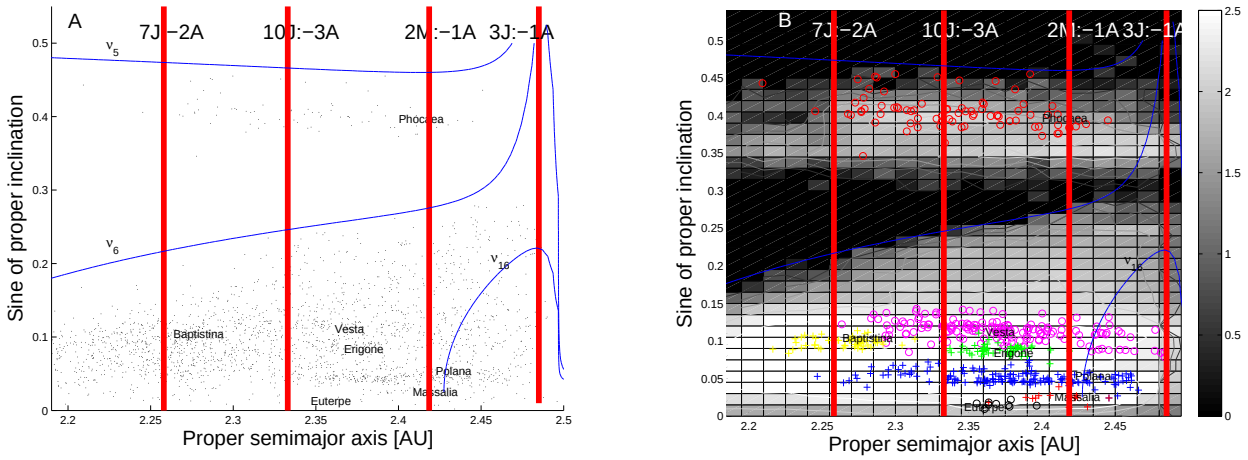

Figure 4. Panel A: An $(a, sin(i))$ projection of inner main belt asteroids in our multi-variate sample. Panel B: contour plot of the number density of asteroids in the proper element sample. Superimposed, we display the orbital location of asteroid families in the CX-complex (plus signs), and in the S-complex (circles).

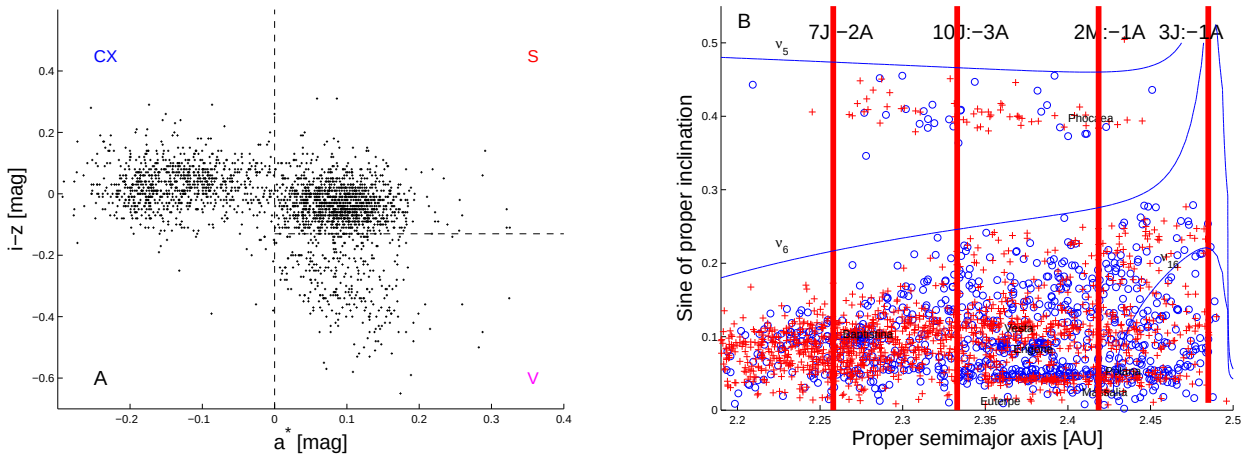

Figure 5. Panel A: an $(a^*, i-z)$ projection of inner main belt asteroids in the in our multi-domain sample. Panel B: an $(a, sin(i))$ projection of the same asteroids, where objects in the CX complex are shown as blue circles, and asteroids in the S-complex are identified as red plus signs.

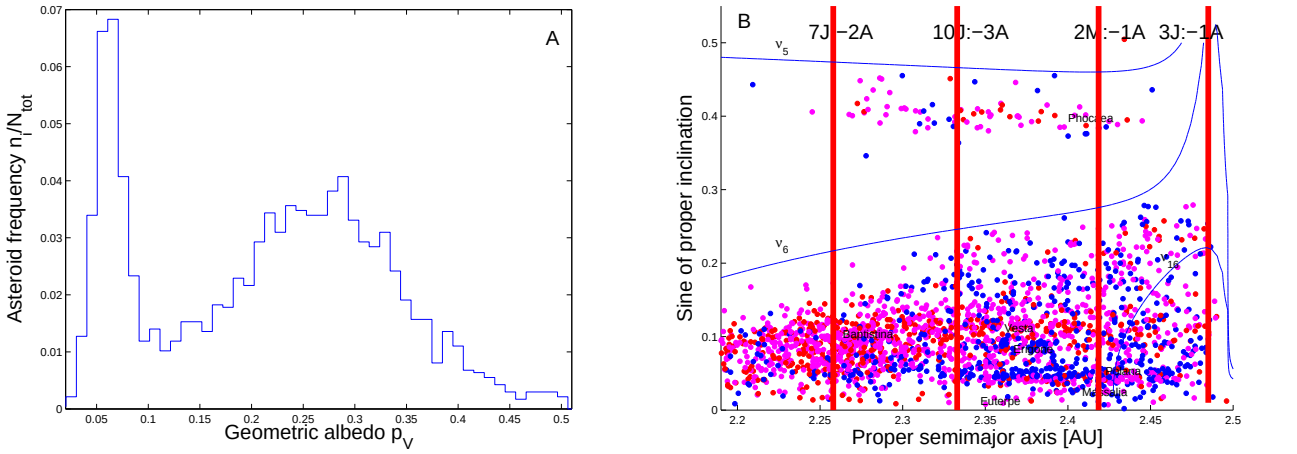

Figure 6. Panel A: a histogram of number frequency values n_i/N_{Tot} as a function of geometric albedo p_V for inner main belt asteroids in our multi-domain sample. Panel B: an $(a, sin(i))$ projection of the same asteroids, where blue full dots are associated with asteroids with $p_V < 0.1$, red full dots display asteroids with $0.1 < p_V < 0.3$, and magenta full dots show asteroids with $p_V > 0.3$.

5.1 The Hestia family

The Hestia family was identified in Nesvorný et al. (2005) as a 154 members group with S-taxonomy at a cutoff in proper element domain of 80 m/s. Here we obtained a CX-halo of 26 members at a cutoff $d_{md} =$ 360 m/s. Eleven objects (42.3% of the total) were SDSS-MOC4 interlopers, and twelve (46.2% of the total) had $p_V < 0.1$.

5.2 The Astraea family

The Astraea family is listed at the AstDyS. We identified a small CX-complex halo of four members at a cutoff of 320 m/s, with no interlopers.

5.3 The Aeolia family

The Aeolia family was identified in Nesvorný et al. (2005) as a group of 28 members at a cutoff of 20 m/s with no identifiable dominant taxonomy. Here we obtained a halo of 14 members at a cutoff $d_{md} =$ 320 m/s, all with CX-complex-taxonomies. Two objects (14.3% of the total) have values of $p_V > 0.1$.

5.4 The Chloris family

The Chloris family was a group of 135 members identified in Nesvorný et al. (2005) at a cutoff in proper element domain of 120 m/s. Most of the members of this group belonged to the C-class. In this work we found a halo of 35 members at a cutoff of 340 m/s. One object (2.9% of the total) was a possible SDSS-MOC4 interloper, and eigth objects (22.9% of the total) had values of $p_V > 0.1$.

5.5 The Misa family

The Misa family was a large C-class group of 119 asteroids identified at a cutoff of 80 m/s in proper element domain by Nesvorný et al. (2005). Here we found a halo of 33 members at a cutoff $d_{md} =$ 355 m/s all belonging to the CX-complex. One object (3.0% of the total) was a possible SDSS-MOC4 and albedo interloper. The Leonidas AstDyS group merges with this family at a cutoff of less than 150 m/s.

5.6 The Brangane family

The Brangane group was a 30 members S-type cluster identified in proper element domain by Nesvorný et al. (2005) at a cutoff of 30 m/s. In this work we identified an S-complex halo of just 3 members at a cutoff $d_{md} =$ 355 m/s. One member (33.3% of the total) was a possible SDSS-MOC4 interloper, and, as observed for some other S-complex families, all objects had $p_V < 0.1$,

5.7 The Bower family

The Bower family was a 82 cluster identified by Nesvorný et al. (2005) at a cutoff of 100 m/s with no dominant taxonomical information. In this work we identified a 27 members halo at a cutoff $d_{md} =$ 260 m/s. Most of the members belonged to the CX-complex, but 6 (22.2% of the total) were possible SDSS-MOC4 interlopers, and 7 objects (25.9% of the total) had $p_V > 0.1$.

5.8 The Cameron family

The Cameron group was identified at a cutoff of 60 m/s by Nesvorný et al. (2005). It was a 162 group made mostly by S-type asteroids. The halo that we identified in this work had 3 members at $d_{md} =$ 310 m/s. Contrary to what was found by Nesvorný et al. (2005), all members have SDSS-MOC4 colors compatible with a CX-complex-taxonomy, but two objects (66.7% of the total) had $p_V > 0.1$. The Innes AstDyS group merges with this family at cutoff lower than 150 m/s.

5.9 The Rafita family

The Rafita family was an S-complex group identified by Nesvorný et al. (2005) in the $(a, e, sin(i))$ proper elements domain at a cutoff of 100 m/s. Unfortunately we could not

identify any member of this family in our multi-domain sample of proper elements, SDSS-MOC4 colors, and geometric albedos. Therefore, we could not analyze this family halo.

5.10 The Eunomia family

The Eunomia family is the largest family in the central main belt. Mothé-Diniz et al. (2005) analyzed the spectra of 43 members of this family, most of which belonging to the S-complex, but with a large taxonomical diversity that suggested surface inhomogeneities or the action of space weathering. The presence of T- and X-class asteroids, classes these compatible with iron meteorites, suggested the possibility that the formation of the Eunomia family may have been the result of the catastrophic break-up of a differentiated (or partially differentiated) parent body. The identification of three V-type asteroids in the orbital proximity of the Eunomia family provided further hints for this possibility. Carruba et al. (2007) showed that it is possible to migrate from the Eunomia dynamical family to the current orbital location of (21238) 1995 WV7, the largest of the V-type asteroids in the Eunomia region, via the interplay of the Yarkovsky effect and the $\nu_5 - \nu_6 + \nu_{16}$ nonlinear secular resonance, on time-scales of at least 2.6 Gyr.

In this work we identified a halo with 52 members, at a cutoff d_{md} of 90 m/s. As found in Mothé-Diniz et al. (2005), the Eunomia family halo is quite diverse, with a predominance of objects belonging to the S-complex, but with a fairly large minority of C- and X-complex asteroids. We found 7 SDSS-MOC4 interlopers and 7 asteroids with $p_V < 0.1$, which yields a percentage of 13.5% likely interlopers. The Planetary Data System group of Schulhof merges with the Eunomia family at a cutoff of 195 m/s.

5.11 The Iannini family

The Iannini family was studied in Nesvorný et al. (2005), where it was identified in proper element domain at a cutoff of 30 m/s. The group was listed as an S-type, but here we found a 93 members halo dominated by CX-complex asteroids, at a cutoff d_{md} of 305 m/s. The discrepancy with Nesvorný et al. (2005) spectral classification may possibly be caused by the low number (18) of objects found in this family at the time. There were no SDSS-MOC4 interloper, and 6 asteroids (6.5% of the total) had $p_V > 0.1$.

5.12 The Gefion family

The Gefion family, previously identified as the Ceres family (Zappalá et al. 1995) and also as the Minerva/Gefion family (Mothé-Diniz et al. 2005), was identified in Mothé-Diniz et al. (2005) as a fairly homogeneous family, with members mostly belonging to the S-complex. Because of its orbital proximity to (1) Ceres, it was studied in Carruba et al. (2003) as a test case for chaotic diffusion caused by close encounters with massive asteroids. The Gefion family halo was identified at a cutoff d_{md} of 210 m/s, with 146 members. Mothé-Diniz et al. (2005) found that the local background of this family is mostly dominated by distinguished C-type asteroids. Indeed our halo is contaminated by a minority of bodies belonging to the C-complex: we found 43 SDSS-MOC4 interlopers and 33 asteroids with $p_V < 0.1$, which yields a percentage of 29.5% and 22.6% likely interlopers, respectively. The Minerva AstDys group merges with this family halo at cutoff lower than 150 m/s.

5.13 The Adeona family

The Adeona family was analyzed by Mothé-Diniz et al. (2005) that found it to be a very homogeneous family, made mostly in its entirety by asteroids belonging to the CX-complex. Because of its orbital proximity to (1) Ceres, it was also studied in Carruba et al. (2003) to understand the long-term effects of diffusion caused by close encounters with massive asteroids. The Adeona family halo has been identified in this work at a cutoff d_{md} of 295 m/s, with 149 members. We found one SDSS-MOC4 interloper (0.7% of the total), and four objects with geometric albedo (barely) larger than 0.1, which corresponds to a percentual of possible interlopers of 2.7%. This high uniformity of the Adeona albedo confirms the results found in Mothé-Diniz et al. (2005).

5.14 The Maria and Renate families

The Maria family was analyzed together with the Renate family in Mothé-Diniz et al. (2005), and both families had a majority of members with known taxonomies belonging to the S-complex, indistinguishable from the local background. Zappalá et al. (1997) analyzed this family and found that the spectra of 10 family members were compatible with those of near-Earth asteroids (433) Eros and (1036) Ganymede, conclusion not supported by the work of Mothé-Diniz et al. (2005). The Maria family halo has been identified in this work at a cutoff of 240 m/s with 135 members. We found 21 objects that can be classified as SDSS-MOC4 interlopers, five of which barely in the area of the CX-complex, and 10 asteroids with $p_V < 0.1$, which yields a percentual of possible interlopers of 15.6% and 7.4%, respectively. The Renate family, considered together with the Maria family in Mothé-Diniz et al. (2005), and also classified as an S-complex group in that work, merges with the Maria family at a cutoff of 225 m/s. For the purpose of halo analysis, the two families can be considered as an unique group.

5.15 The Padua family

This family, previously associated to the asteroid (110) Lydia, is made mostly by X-type asteroids indistinguishable from the local background, according to Mothé-Diniz et al. (2005). The family is very important from a dynamical point of view, since it is the second family, after the Agnia, to have most of its members in a nonlinear secular resonance configuration. More than 75% of its members, according to Carruba (2009a), are currently in a z_1 librating state. Conservation of the $K_2^{'} = \sqrt{2 - e^2}(2 \cos i)$ quantity associated with this secular allowed to set limits on the original ejection velocity field, that was in agreement with result obtained with an alternative Monte Carlo model that included Yarkovsky and YORP semi-major axis mobility. The current spread of values in the $(\sigma, g - g_6 + s - s_6)$ plane, where σ is the resonant

argument of the z_1 resonance allowed to set a lower limit on the age of the family of 25 Myr, that was then used to set an upper limit on the effect of low-energy collisions. The Padua halo was identified at a cutoff of 130 m/s, with 31 members, and no interlopers. The Zdenekhorsky AstDyS group merges with the Padua halo at cutoff lower than 100 m/s.

5.16 The Juno family

The Juno family was identified in Nesvorný et al. (2005) as a 74 members S-type group. Here we identified a halo of 61 members at a cutoff of 275 m/s, that, contrary to what published in Nesvorný et al. (2005), is made mostly by CX-complex bodies, with (3) Juno itself, an Sk object, a possible interloper. There were no SDSS-MOC4 interlopers, and 4 asteroids (6.6% of the total) had values of $p_V > 0.1$.

5.17 The Dora family

The Dora family was classified by Mothé-Diniz et al. (2005) as a very homogeneous C-complex family, with the majority of members belonging to the Ch class, and five objects in the C and B classes. The family was very differentiated from the local background, made mostly by asteroids belonging to the S-complex. The Dora halo was identified at a cutoff of 265 m/s, with 108 members. Only 2 members were possible SDSS-MOC4 interlopers and had $p_V > 0.1$ (1.9%), confirming the very homogeneous nature of this family, as found in Mothé-Diniz et al. (2005).

5.18 The Merxia and Nemesis family

The Merxia family was found to be made mostly by S-complex asteroids in Mothé-Diniz et al. (2005), and was dominated by the two largest bodies, (808) Merxia, and (1327) Namaqua, the second of which was most likely an interloper because of its low albedo. The family is crossed by the 3J:-1S:-1A three-body mean-motion resonance, which divides it into two lobes and cause a depletion in the number of members at the center of the family, and it was well differentiated from the local background, dominated by CX-complex objects, according to Mothé-Diniz et al. (2005). Nesvorný et al. (2005) also identified in the region the Nemesis family, but its halo merges with that of the Merxia family at a cutoff of $\simeq 200$ m/s, and we therefore decided to treat the two families as a single case. We found a CX-halo at a cutoff of 250 m/s, with 19 members, 5 of which could be SDSS-MOC4 interlopers and 9 of which have $p_V < 0.1$. The large percentual of possible interlopers (26.3% and 42.1%) may be caused by the fact that, possibly, there is no Merxia halo, and the family is small and limited to the S-complex core found in Mothé-Diniz et al. (2005)

5.19 The Agnia family

The Agnia family, previously identified as the Liberatrix family, was the first group to be found having the majority of its members in z_1 librating states (Vokrouhlický et al. 2006b). Conserved quantities of the z_1 resonance and spread in the $(\sigma, g-g_6+s-s_6)$ plane, as discussed for the case of the Padua family, were introduced in that work to obtain constraints on the family original ejection velocity field and age. The family, first analyzed by Bus (1999), appears compatible with an S-complex taxonomy in Mothé-Diniz et al. (2005), while the local background is dominated by CX-complex bodies. Here we determined a halo at a cutoff of 190 m/s, with 12 members. As for the Merxia family halo, we found a large number of possible interlopers: 4 SDSS-MOC4 CX-complex members, and 4 $p_V < 0.1$ asteroids (33.3% of the total), which may suggest that the actual Agnia family is small and with a limited halo.

5.20 The Astrid family

The Astrid family was identified in Bus (1999) and Mothé-Diniz et al. (2005) as a very tight clump, with most members belonging to the C-complex. No asteroid in the local background had taxonomical information at the time of Mothé-Diniz et al. (2005) analysis. Here we found a very robust and isolated group, with a halo that was separated from the local background for cutoffs as large as 435 m/s, with 6 members, and no interlopers, confirming that this is a very homogeneous and robust group.

5.21 The Hoffmeister family

The Hoffmeister family was found to be a very compact and spectrally homogeneous CX-group in Mothé-Diniz et al. (2005). Here we determined a halo with 62 members at a cutoff of 210 m/s. No interlopers were detected, so confirming previous analysis of this group.

5.22 The Lavrov family

The Lavrov group, previously known as the Henan clump, is a small group formed mostly by L-type asteroids, that are also typical of the local background (Mothé-Diniz et al. 2005). We identified a halo of 8 members at a cutoff of 200 m/s. We identified only 1 possible SDSS-MOC interloper and 2 asteroids with $p_V < 0.1$ (12.5% and 25.0% of the total, respectively), which confirms that this should be a fairly compact and robust L-class group.

5.23 The 1995 SU37 family

The 1995 SU37 group is listed at the Planetary Data System. We identified a small S-complex halo of four members, at a cutoff of 105 m/s, with no interlopers.

5.24 The Watsonia family

The Watsonia family is listed at the AstDyS. We identified a CX-complex halo of ten members at a cutoff of 425 m/s. Three objects (30.0% of the total) were possible SDSS-MOC4 interlopers, and 5 objects (50% of the total) had $p_V > 0.1$.

5.25 The Ino, Atalante, and Anacostia families

The Ino, Atalante, and Anacostia families are listed at the AstDyS. Unfortunately we could not find any of their members in our multi-domain database. No information is therefore available for this family in this work.

5.26 The Gersuind family

With the Gersuind family we start the analysis of the highly inclined $\sin i > 0.3$ asteroid groups in the central main belt, that were the subject of the study of Carruba (2010b). The Gersuind family was studied in Gil-Hutton (2006). While having most of its members at $\sin i > 0.3$, it lies at lower inclinations than the center of the ν_6 resonance, and it is not therefore considered a proper high-inclination family by other authors, such as Machuca and Carruba (2011). The few objects with SDSS-MOC 3 data in the family obtained by Carruba (2010b) were compatible with an S-complex taxonomy. Here we found a halo at 310 m/s with 7 members, the majority of which were compatible with an S-complex taxonomy. Three objects (42.9% of the total) were SDSS-MOC4 interlopers, and 2 objects (28.6% of the total) had albedos smaller than 0.1, confirming the analysis of Carruba (2010b). The Planetary Data System Emilkowalski group merges with this family at cutoff lower than 100 m/s.

5.27 The Myriostos family

The Myriostos family is listed at the AstDyS. We identified a 7 members CX-complex halo at a cutoff of 580 m/s, with two SDSS-MOC4 interlopers (28.6% of the total). Six objects (85.7% of the total) have $p_V > 0.1$.

5.28 The Kunitaka family

The Kunitaka family is listed at the AstDyS. We could not find any of its members in our multi-domain database, so no information is available on this group in this work.

5.29 The Hansa family

The Hansa family is the largest dynamical group among high inclination families in the central main belt. The Hansa family was originally proposed by Hergenrother et al. (1996), studied in Gil-Hutton (2006), and re-analyzed in Carruba (2010b), that found a large group compatible with an S-type taxonomy. The family is located in a stable island limited in inclination by the ν_6 and ν_5 linear secular resonances. This is confirmed by our analysis: we found a 20 members halo at a cutoff of > 535 m/s (at cutoff as large as 1000 m/s the family does not yet connect with the local background), with all but one member (95% of the total) with an S-complex taxonomy. We did not detected asteroids with $p_V < 0.1$. The 2001 YB113 AstDyS group merges with this family halo for cutoff less than 150 m/s.

5.30 The Brucato family

The Brucato family was first identified as a clump in proper elements domain and as a family in the $(n, g, g + s)$ proper frequencies domain in Carruba (2010b) [4]. Novaković et al. (2011) then re-obtained this group in proper element domains as a family, using a larger sample of asteroid proper elements. The family is located in a stable island limited in inclination by the ν_5 and ν_{16} linear secular resonances. The group was made mostly by CX-complex asteroids, and this is confirmed by the current analysis: we identify a family halo at a cutoff of 950 m/s with 32 members, all belonging to the CX-complex. Two albedo interlopers (6.3% of the total) were identified in this family halo. The 1998 DN2, 1999 PM1, 1998 LF3, and 2004 EW7 AstDyS groups merge with this family at cutoffs lower than 150 m/s.

5.31 The Dennispalm family

The Dennispalm family is listed at the AstDys. We could not find any of its members in the multi-domain database, so no information is available on this group in this work.

5.32 The Barcelona family

The Barcelona family was first identified as a clump in Gil-Hutton (2006). Carruba (2010b) identified the group as a dynamical family, and this was confirmed by the later work of Novaković et al. (2011). The Barcelona family was made mostly by Sq asteroids. Very few objects were present in our multi-domain sample of asteroids at this inclinations: we identified an S-complex halo of only one member at a cutoff of 730 m/s.

5.33 The Tina family

The Tina family, first identified in Carruba (2010b), is unique in the Solar System because all of its members are in ν_6 anti-aligned librating states, making it the only family currently known to lie in a stable island of a linear secular resonance. Carruba and Morbidelli (2011) studied its dynamics and obtained estimates of the family age and possible survival time before the family members escape from the stable island (both events happened and will happen on timescales of 150 Myr). (1222) Tina itself belongs to the X-complex. The one halo object that we identified at a cutoff of 890 m/s is compatible with such taxonomy. The very limited number of objects with known taxonomy does not, however, allow to determine if the Tina's group is a real family or a conglomerate of asteroids happening to be lying in the local stable island, yet.

5.34 The Gallia family

The Gallia family was first identified as a clump in Gil-Hutton (2006), and was re-obtained as a family in Carruba (2010b), and Novaković et al. (2011). It is located in a stable island limited in inclination by the ν_5 and ν_{16} linear secular resonances. Its taxonomy was compatible with an S-complex composition, according to the analysis of Carruba (2010b). Here we identified a halo of just three members at a cutoff of

[4] See Carruba and Michtchenko (2007) for a more in depth discussion of frequency families.

$> 410\ m/s$. All members were compatible with an S-complex taxonomy.

5.35 The Pallas family

Williams (1992) first proposed the Pallas family, that was later re-analyzed by Gil-Hutton (2006), Carruba (2010b), and and Novaković et al. (2011). Most of the Pallas family members have B-type taxonomies, but C-type objects are also observed in the orbital region. In this work we identified a halo of 8 members at a cutoff of $> 920\ m/s$. No SDSS-MOC4 interloper was found, but, as observed for Hungaria family members, all 8 asteroids have large values of p_V, in principle incompatible with a B- or C-type taxonomy.

5.36 The central main belt: an overview

Our results for the central main belt are summarized in Table 3, that has the same format as Table 2.

Fig. 7, panel A, displays an $(a, sin(i))$ projection of asteroids in our multi-variate sample in the central main belt. Blue lines show the location of the main linear secular resonances, using the second order and fourth-degree secular perturbation theory of Milani and Knežević (1994) to compute the proper frequencies g and s for the grid of (a, e) and $(a, \sin(i))$ values shown in Fig. 10, panel A, and the values of angles and eccentricity of (480) Hansa, the highly inclined asteroid associated with the largest family in the region (Carruba 2010b). Other symbols have the same meaning as in Fig. 4, panel A. In panel B of the same figure we display a density map of the central main belt. We computed the log_{10} of the number of all asteroids with proper elements per unit square in a 22 by 67 grid in a (starting at $a = 2.500$ AU, with a step of 0.015 AU) and $sin(i)$ (starting at 0, with a step of 0.015). Superimposed to the density map, we also show the orbital projection of the halos found in this work shown as red plus signs for CX-complex families and as blue circles for S-complex families. The other symbols have the same as in Fig. 10, panel B. The reader may notice that regions with higher number density of asteroids are associated with the families halos found in this work. The halos that we determined do not have multiple membership, i.e., an asteroid in a given family halo is not present in another family halo.

Fig. 8 displays a projection in the $(a^*, i - z)$ plane of all asteroids in our multi-domain sample (panel A), and an $(a, sin(i))$ projection of the same asteroids, (panel B). We refer the reader to the caption of Fig. 6 for a more detailed description of this figure symbols. The central main belt is a transitional region, where CX-complex and S-complex asteroids are rather mixed. A greater proportion of S-type asteroids can be found at lower semi-major axis (and vice-versa), but overall, no group dominates the local taxonomy.

This is confirmed by an analysis of WISE p_V geometrical albedo data, a histogram of which is presented in Fig. 9, panel A. Fig. 9, panel B, displays an $(a, sin(i))$ projection of the same asteroids, where we used the same color code as in Fig. 6, panel B.

One can notice the clearly bi-modal distribution of asteroid albedos, and the mixture of objects with low albedo and high albedo that dominates the central main belt. Having analyzed the families of the central main belt, we are now ready to move on to the outer main belt.

6 OUTER MAIN BELT

The outer main belt is dynamically limited in semi-major axis by the 5J:-2A and 2J:-1A mean-motion resonances (Zappalá et al. 1995). The linear secular resonance ν_6 separates the low-inclined asteroid region from the highly inclined area, dominated by the Euphrosyne family (Machuca and Carruba 2011). We found 5385 objects that have proper elements and frequencies, SDSS-MOC4 colors, WISE geometric albedo data, and satisfy our error analysis criteria in the outer main belt. We start our analysis of families halos by investigating the Koronis family.

6.1 The Koronis family

The Koronis family is one of the most interesting families in the main belt. Bottke et al. (2002) explained its shape in eccentricity as originating by the interaction of asteroids evolving via Yarkovsky effect into secular resonances such as the $2\nu_5 - 3\nu_6$. Carruba and Michtchenko (2007) showed that its upper boundary in eccentricity is limited by the $\nu_6 + 2\nu_5 - 2\nu_7 + \nu_{16}$ nonlinear secular resonance. The interesting subgroup of the Karin cluster, identified by Nesvorný et al. (2002a) opened new perspectives in the understanding of recent breakups among asteroids. Mothé-Diniz et al. (2005) identified this family as predominantly belonging to the S-complex, with a few interlopers belonging to the C- and D-types, that predominate in the background. The presence of a few K-type asteroids in the family was somehow puzzling, and justified by Mothé-Diniz et al. (2005) as a possible remnant of a pre-existing family.

In this work we identified a halo with 200 members, at a cutoff d_{md} of 215 m/s. 32 of the halo members have SDSS-MOC4 colors not compatible with an S-complex taxonomy, which yields to a 16.0% fraction of possible interlopers in the halo, somewhat in agreement with the finding of Mothé-Diniz et al. (2005). About 14 asteroids (7.0% of the total) have values of p_V smaller than 0.1, which is the limit for S-complex asteroid albedos, and that may be related with the presence of the interloper population found in Mothé-Diniz et al. (2005).

6.2 The Lau family

The Lau cluster is listed at the Planetary Data System. In this work we identified a 10 objects CX halo at a cutoff of 490 m/s. No interloper was found in this group.

6.3 The (1993) FY12 family

The cluster around (18405) (1994 FY12) was identified for the first time in Nesvorný et al. (2005) at a cutoff of 50 m/s as an 11 asteroids X group. Here we find a halo at a cutoff d_{md} of 355 m/s of just 2 members, one of which (50.0% of the total) have $p_V > 0.1$. The possible X-type composition of this small group appears to be confirmed by our analysis.

Table 3. Asteroid families halos in the central main belt.

First halo member	d_{md} cutoff value $[m/s]$	Number of members	Spectral Complex	Number of SDSS-MOC4 likely interlopers	Number of p_V likely interlopers
(46) Hestia: (7321)	360	26	CX	11	12
(5) Astraea: (4018)	320	4	CX	0	0
(396) Aeolia: (76144)	320	14	CX	0	2
(410) Chloris: (9545)	340	35	CX	1	8
(569) Misa: (2289)	355	33	CX	1	1
(606) Brangane: (56748)	355	3	S	1	3
(1639) Bower: (26703)	260	27	CX	6	7
(2980) Cameron: (4067)	310	3	CX	0	2
(15) Eunomia: (630)	90	52	S	7	7
(4652) Iannini: (143366)	305	93	CX	0	6
(1272) Gefion: (2373)	210	146	S	43	33
(145) Adeona: (1783)	295	149	CX	1	4
(170) Maria/Renate: (4104)	240	135	S	21	10
(363) Padua: (2560)	130	31	CX	0	0
(3) Juno: (22216)	275	61	CX	0	4
(668) Dora: (1734)	265	108	CX	2	2
(808) Merxia/Nemesis: (3439)	250	19	CX	5	8
(847) Agnia: (1020)	190	12	S	4	4
(1128) Astrid: (2169)	435	6	CX	0	0
(1726) Hoffmeister: (1726)	210	62	CX	0	0
(2354) Lavrov: (2354)	200	8	S	1	2
(18466) 1995 SU37: (95534)	105	4	S	0	0
(729) Watsonia: (5492)	425	10	CX	3	5
(686) Gersuind: (14627)	310	7	S	3	2
(10000) Myriotos: (101897)	580	7	CX	2	6
(480) Hansa: (13617)	> 535	20	S	1	0
(4203) Brucato: (4203)	950	32	CX	0	2
(945) Barcelona: (11028)	730	1	S	0	0
(1222) Tina: (16257)	890	1	CX	0	0
(148) Gallia: (40853)	> 410	3	S	0	0
(2) Pallas: (24793)	> 920	8	CX	0	8

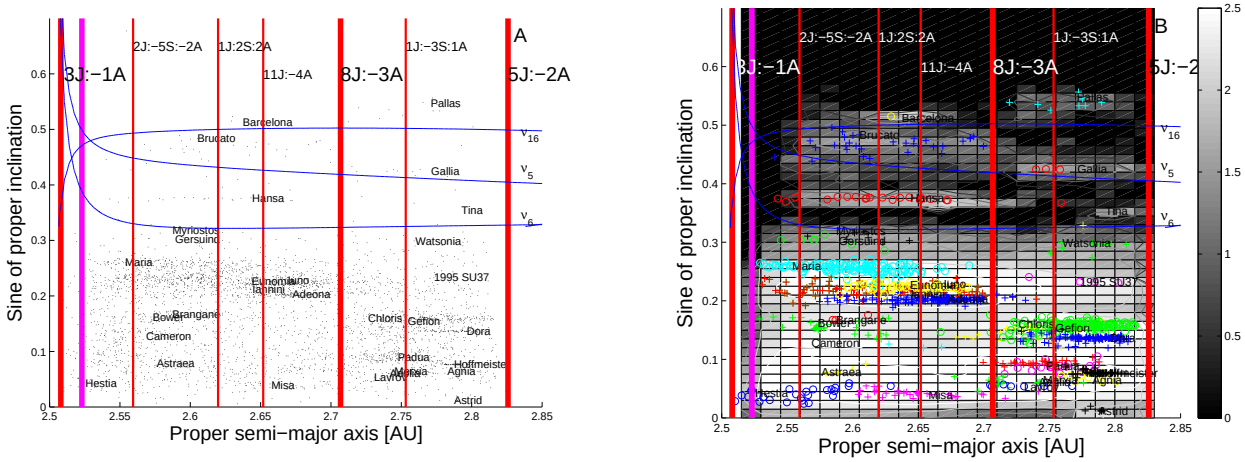

Figure 7. Panel A: An $(a, sin(i))$ projection of central main belt asteroids in our multi-variate sample. Panel B: contour plot of the number density of asteroids in the proper element sample. Superimposed, we display the orbital location of asteroids of families in the CX-complex (plus signs) or in the S-complex (circles).

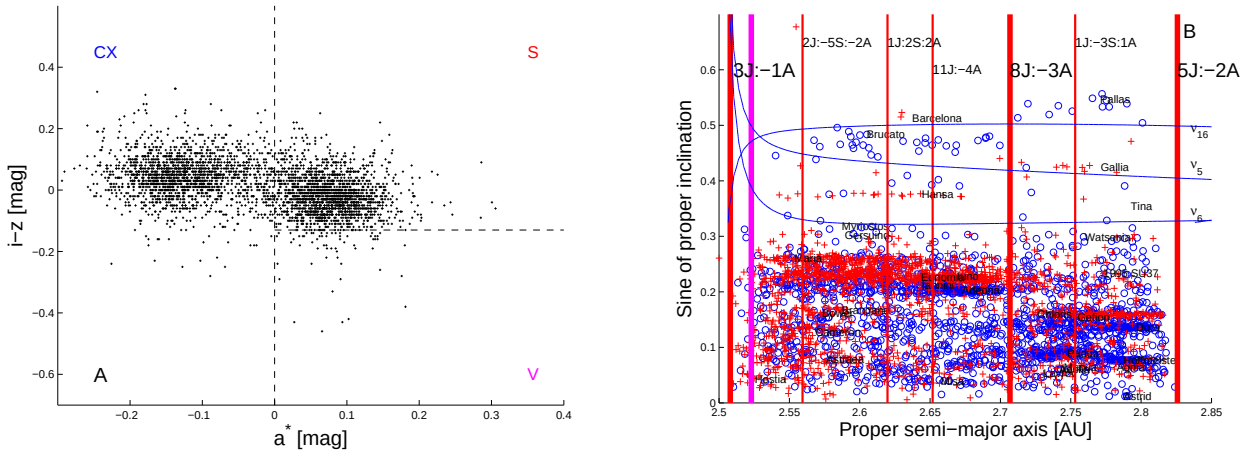

Figure 8. Panel A: an $(a^*, i-z)$ projection of central main belt asteroids in our multi-domain sample. Panel B: an $(a, sin(i))$ projection of the same asteroids, where objects in the CX complex are shown as blue circles, and asteroids in the S-complex are identified as red plus signs.

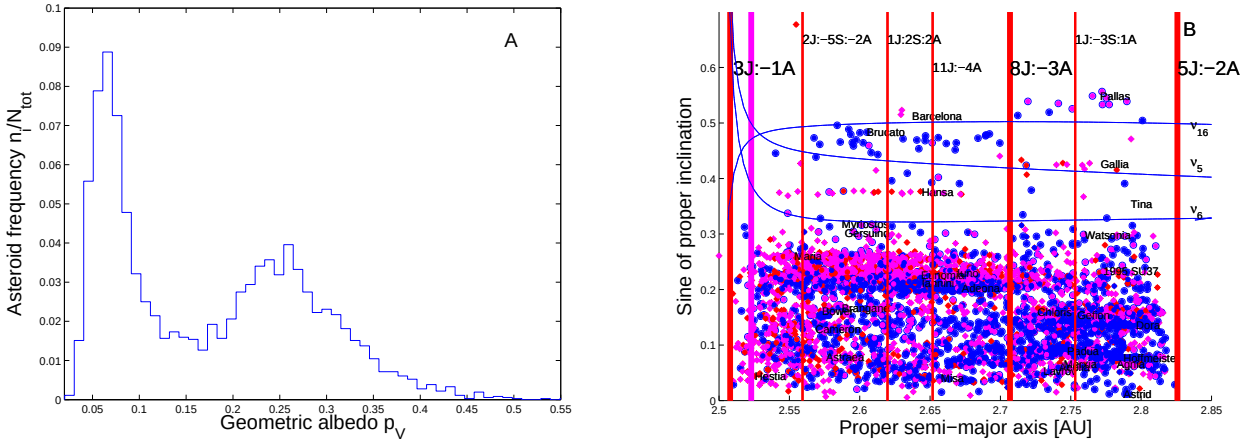

Figure 9. Panel A: a histogram of number frequency values n_i/N_{Tot} as a function of geometric albedo p_V for central main belt asteroids in our multi-domain sample. Panel B: an $(a, sin(i))$ projection of the same asteroids, where blue full dots are associated with asteroids with $p_V < 0.1$, red full dots display asteroids with $0.1 < p_V < 0.3$, and magenta full dots show asteroids with $p_V > 0.3$.

6.4 The Fingella family

The Fingella family is listed at the Planetary Data System. In this work we identified a 16 objects CX halo at a cutoff of 480 m/s. No interloper was found in this group.

6.5 The Naema family

The Naema group is another family discussed in Nesvorný et al. (2005), where it was visible at a cutoff of 40 m/s as a 64 C-type group. Here we found a halo of 43 members at a cutoff of 390 m/s, with all members belonging to the CX-complex. No interlopers were found in this group.

6.6 The Brasilia family

The Brasilia family was identified as a small clump of 96 members in Mothé-Diniz et al. (2005), of which only 4 had known spectral type, all belonging to the CX-complex. We identified a small halo of 24 objects, most belonging to the CX-complex, that merges with the local background at a cutoff of 440 m/s. While all but 3 halo members (12.5% of the total) have SDSS-MOC4 colors compatible with a taxonomy in the CX-complex, the vast majority of these asteroids (17, 70.8% of the total) has large albedos ($p_V > 0.1$), not usually associated with a CX-composition. The reason for the large albedo values of these objects remains unexplained.

6.7 The Themis family

The Themis family is a rather large, homogeneous group, made mostly by asteroids of types belonging to the C/X-complex. Mothé-Diniz et al. (2005) discuss that the spectral type of the family members is not distinguishable from that of asteroids in the background, that is dominated by C and X-type objects. Tanga et al. (1999) suggests that this family originated from the break-up of a large ($\simeq$ 370 km in diameter) C-type parent body. In this work we identified a halo with 700 members, at a cutoff d_{md} of 310 m/s. 9 of the halo members have SDSS-MOC4 colors not compatible with a C/X-complex taxonomy, which yields a 1.3% fraction of

possible interlopers in the halo. 50 asteroids have values of p_V larger than 0.1, which is the limit for CX-complex asteroid albedos, which yields a percentage of possible albedo interlopers of 7.1%. The AstDys Ashkova group merges with the Themis halo at a cutoff of 205 m/s.

6.8 The Eos family

Vokrouhlický et al. (2006b) studied in detail the dynamical evolution of this asteroid family, also pioneering the use of Monte Carlo methods for asteroid families chronology. The Eos family is crossed by the powerful 9J:-4A mean-motion resonance, and interacts with the z_1, $2\nu_5 - 3\nu_6$ and $2\nu_5 - 2\nu_6 + \nu_{16}$ secular resonances (see also Carruba and Michtchenko 2007). More recently, Brož and Morbidelli (2013) identified Eos halo members based on SDSS-MOC4 data, and obtained an estimate of the halo age, that is in agreement with what found by Vokrouhlický et al. (2006b). In this work we identified a halo at a cutoff of 165 m/s, with 738 members. In agreement with what was found by Mothé-Diniz et al. (2005), the taxonomy of the family is quite inhomogeneous, but well distinguished from the local background that is dominated by C and X asteroids. Most members of the Eos family have a characteristic K-type taxonomy, and we found that many members of the halo members have $(a^*, i-z)$ colors compatible with an S-complex taxonomy. But, as discussed in Sect. 3, the Eos family lies at the separation between CX-complex and S-complex asteroids in the $(a^*, i-z)$. Our simple criterion for identifying S-complex asteroids, $a^* > 0$, does not apply well to the case of the Eos family. 379 asteroids (51.4% of the total) have values of $a^* < 0$ and may be considered interlopers. 132 Eos halo asteroids have values of $p_V < 0.1$, which yields that 17.9% of the halo asteroids may actually be albedo interlopers. The quite diverse mineralogy of bodies in the Eos family area provides challenges that should be confronted with more advanced tools than the one used in this paper, in our opinion. The Telramund cluster, that was identified as an S-type 70 members group at a cutoff of 60 m/s by Nesvorný et al. (2005), merges at very low cutoff with the Eos family, so we consider this group as a substructure of the larger family.

6.9 The Hygiea family

(10) Hygiea is the fourth most massive asteroid of the main belt, and the family associated with this body has been studied in Zappalá et al. (1995), Mothé-Diniz et al. (2005), and, more recently by Carruba (2013). It is made mostly by bodies belonging to the CX-complex, and, as the Themis family, is not easily distinguishable from the local background of objects. We identified a halo with 426 objects at a cutoff of 290 m/s. The slightly higher number of objects that we found in the Hygiea halo with respect to Carruba (2013) migth be due to the larger sample of bodies in our data-set. Of the 426 possible halo members, 6 (1.4%) may be interlopers based on SDSS-MOC4 colors analysis, and 36 have $p_V > 0.1$, that is incompatible with CX-complex asteroids. Overall, we found a maximum of 8.5% of objects that are possibly not correlated with the Hygiea halo. The AstDys Filipenko group merges with this family halo at a cutoff of 125 m/s.

6.10 The Emma family

The Emma family was identified by Nesvorný et al. (2005) as a 76 members group at a cutoff of 40 m/s in proper elements domain. No information on its taxonomy was given in that article. In this work we found a family halo of 43 members at a cutoff d_{md} of 270 m/s. No interlopers were identified in this family halo.

6.11 The Veritas family

The Veritas family is a relatively small group, made mostly by CX-complex asteroids. Milani and Farinella (1994) used for the first time chaotic chronology on this family to determine its relatively young age, later confirmed by other works. We identified a halo of 148 members at a cutoff of 240 m/s. 2 objects have colors not compatible with a CX-complex taxonomy, and 9 had values of $p_V > 0.1$. Overall, up to 6.1% of the halo members encountered may be interlopers of the Veritas halo.

6.12 The Lixiaohua family

The Lixiaohua family was identified by Nesvorný et al. (2005) as a 97 CX-complex group at a cutoff of 50 m/s. It was the subject of a dynamical study by Novaković et al. (2010) that extensively studied the local dynamics and the diffusion in the (e_p, i_P) plane using Monte Carlo modeling. In this work we identified a 69 members CX halo at a cutoff of $d_{md} = 255$ m/s. Only one object (1.4% of the total) was a possible SDSS-MOC4 interloper, and all asteroids in the halo had $p_V < 0.1$. The AstDyS Gantrisch group merges with this family at cutoffs lower than 50 m/s.

6.13 The Aegle family

The Aegle family is an AstDyS group. We identified a 21 CX-complex group at a cutoff of 290 m/s. Two objects (9.5% of the total) were possible SDSS-MOC4 interlopers, and all members had low albedos.

6.14 The Meliboea family

The Meliboea family was discussed by Zappalá et al. (1995) and Mothé-Diniz et al. (2005). It is a small group, mainly composed by asteroids belonging to the CX-complex. It is a rather inclined family ($i_p \simeq 15^\circ$), characterized by the presence of several weak mean-motion and secular resonances. We identified a halo with 73 members at a cutoff of 270 m/s. As found by Mothé-Diniz et al. (2005), the Meliboea family is fairly homogeneous, with only three members of the halo with colors not compatible with a CX-complex taxonomy. Only one halo member has $p_V > 0.1$, which yields a percentage of up to 4.1% possible interlopers. The AstDyS group of Inarradas merges with this family halo at a cutoff of 140 m/s, while the Traversa cluster is englobed at a cutoff of 205 m/s.

6.15 The Klumpkea/Tirela family

The Klumpkea family was identified in Machuca and Carruba (2011) and corresponds to the old Tirela family of Nesvorný et al. (2005). Nesvorný et al. (2005) listed the Tirela family as a D-group. Here we found a halo at a cutoff of 290 m/s with 21 members, 2 of which (9.5% of the total) have colors (barely) in the S-complex area. All members of the halo have $p_V < 0.1$, which makes this family compatible with a C-complex taxonomy. The AstDyS Zhvanetskij cluster is annexed by this halo at a cutoff of 165 m/s, the Ursula family is englobed at 200 m/s, and the Pannonia group merges at a cutoff of 245 m/s.

6.16 The Theobalda family

The Theobalda family is also an AstDyS group. We identified a 34 members CX-complex halo, with two (5.9% of the total) possible albedo interlopers.

6.17 The Kartvelia family

The Kartvelia family is listed at the AstDyS. We found a 26 members CX-complex halo at a cutoff of 280 m/s, with just one (3.8% of the total) possible SDSS-MOC4 interloper.

6.18 The Alauda family region

The orbital region of the Alauda family has been most recently analyzed by Machuca and Carruba (2011) that found several small groups, among which the Alauda and Luthera families, in the area. In this work we identified a 158 CX-complex group at a cutoff of 420 m/s. Two members, 1.3% of the total, have colors in the S-complex region, and 19 objects, 12.0% of the total, have $p_V > 0.1$. The AstDys Higson cluster merges with this halo at a cutoff of 235 m/s, the AstDyS Moravia and Snelling groups merge at a cutoff of 240 m/s, while the AstDyS Vassar cluster is annexed at 255 m/s.

6.19 The Euphrosyne family

Machuca and Carruba (2011) most recently analyzed the orbital region of this highly inclined asteroid family. This family is characterized by its interaction with linear secular resonances. In particular, 13 of its members are in ν_6 anti-aligned librating states, one in a ν_5 anti-aligned librating state (242435), and one in a ν_5 aligned librating state (2009 UL136), according to Machuca and Carruba (2011). The long-term effect of close encounters of asteroids with absolute magnitude $H < 13.5$ with (31) Euphrosyne was recently studied in Carruba et al. (2013). As discussed in Machuca and Carruba (2011), the Euphrosyne family is separated by the near regions of (69032) and Alauda in inclination by areas with very low asteroid densities. It is a region with a relatively small population of objects, separated among them by large distances, which explains why the 75 members halo that we identified in this work is encountered at the high cutoff value of 575 m/s. All halo members have colors in the S-complex area, and three members have $p_V > 0.1$. As for the case of the Klumpkea family, this is a group highly compatible with a C-complex taxonomy, with a 4.0% of possible interlopers.

6.20 The outer main belt: an overview

Having obtained estimates for the halos of the main families in the outer main belt, we are now ready to outline our results. As done for previous asteroid regions, our results are summarized in Table 4.

Fig. 10, panel A, displays an $(a, sin(i))$ projection of asteroids in our multi-variate sample in the outer main belt, with the same symbols used for analogous figure in the inner and central main belt. Here, however, blue lines show the location of the main linear secular resonances, using the second order and fourth-degree secular perturbation theory of Milani and Knežević (1994) to compute the proper frequencies g and s for the grid of (a, e) and $(a, \sin(i))$ values shown in Fig. 10, panel A, and the values of angles and eccentricity of (31) Euphrosyne, the highly inclined asteroid associated with the largest family in the region (Machuca and Carruba 2011). In panel B of the same figure we display a density map of the outer main belt. To quantitatively determine the local density of asteroids, we computed the log_{10} of the number of all asteroids with proper elements per unit square in a 67 by 67 grid in a (starting at $a = 2.805$ AU, with a step of 0.015 AU) and $sin(i)$ (starting at 0, with a step of 0.015). The other symbols are the same as in Fig. 4, panel A. The reader may notice that regions with higher number density of asteroids are associated with the families halo found in this work. Families halos are indeed more extended in proper elements domain than the core families found with the standard HCM.

To study how the family halos found in this work are related to the local taxonomy, we also plotted in Fig. 11 a projection in the $(a^*, i - z)$ plane of all asteroids in our multi-domain sample (panel A), and an $(a, sin(i))$ projection of the same asteroids, (panel B). The great majority of asteroids in the region belong to the CX-complex, but there is a sizable minority of bodies belonging to the S-complex, that, as shown in Fig. 11, panel B, are mostly associated with the Eos and Koronis families.

This is confirmed by WISE p_V geometrical albedo data, a histogram of which is presented in Fig. 12, panel A. Fig. 12, panel B, displays an $(a, sin(i))$ projection of the same asteroids, with the color code used in Fig. 6, panel B. The great majority of objects have low albedos, characteristics of the dark C-type objects that predominates in the outer main belt, but there is a fraction of asteroids, that are associated with the Eos and Koronis families, with medium and high values of geometric albedo.

Overall, we confirmed the results of the taxonomical analysis of Mothé-Diniz et al. (2005): the outer main belt is dominated by CX-complex dark asteroids, with the two notable exceptions of the Eos and Koronis families. S-complex asteroids in the local background may be escapers from these two large families. Dynamical studies on the orbital evolution of members of these families are however needed to confirm this conclusion.

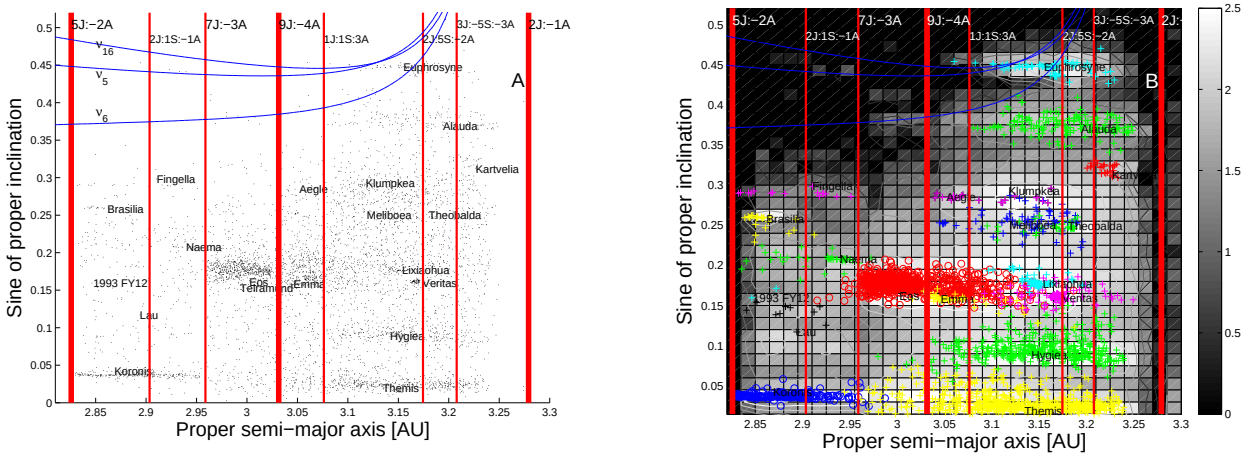

Figure 10. Panel A: An $(a, sin(i))$ projection of outer main belt asteroids in our multi-variate sample. Panel B: contour plot of the number density of asteroids in the proper element sample. Superimposed, we display the orbital location of asteroids of families in the CX-complex (plus signs) or in the S-complex (circles).

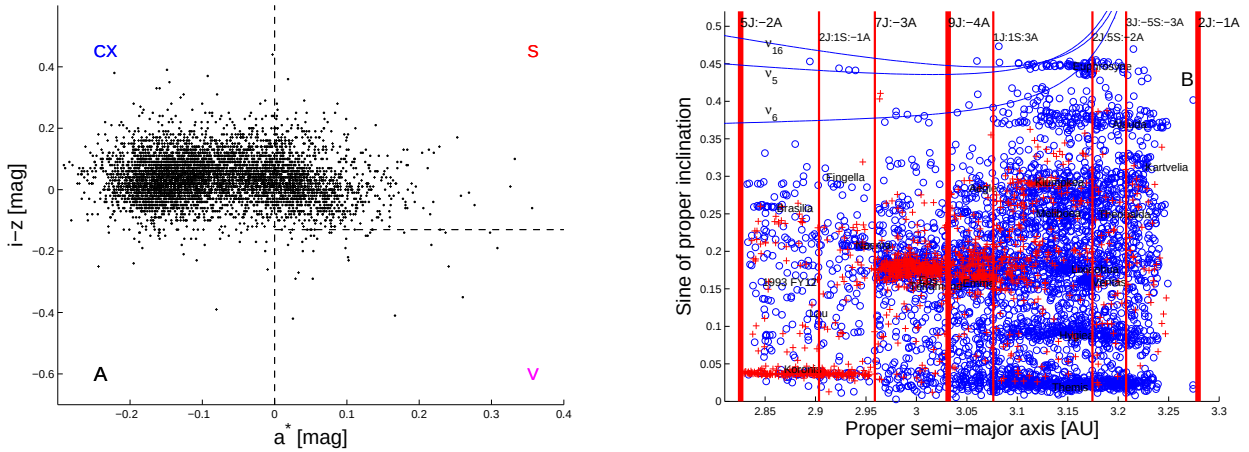

Figure 11. Panel A: an $(a^*, i-z)$ projection of outer main belt asteroids in our multi-domain sample. Panel B: a $(a, sin(i))$ projection of the same asteroids, where objects in the CX complex are shown as blue circles, and asteroids in the S-complex are identified as red plus signs.

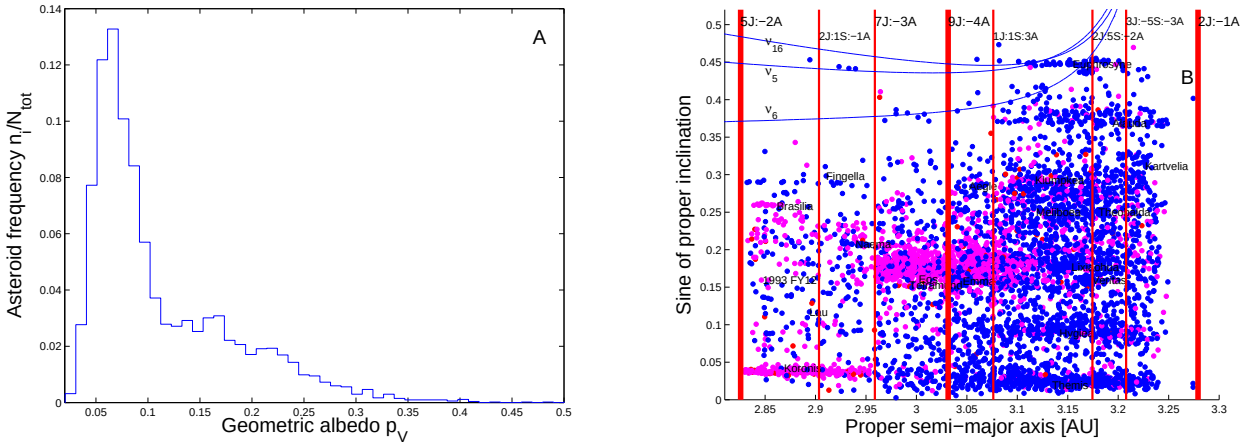

Figure 12. Panel A: a histogram of number frequency values n_i/N_{Tot} as a function of geometric albedo p_V for outer main belt asteroids in our multi-domain sample. Panel B: an $(a, sin(i))$ projection of the same asteroids, where blue full dots are associated with asteroids with $p_V < 0.1$, red full dots display asteroids with $0.1 < p_V < 0.3$, and magenta full dots show asteroids with $p_V > 0.3$.

Table 4. Asteroid families halos in the outer main belt.

First halo member	d_{md} cutoff value $[m/s]$	Number of members	Spectral likely interlopers	Number of SDSS-MOC4 Complex	Number of p_V likely interlopers
(158) Koronis: (761)	215	200	S	32	14
(18405) 1993 FY12: (29959)	355	2	CX	0	1
(10811) Lau: (51707)	490	10	CX	0	0
(709) Fingella: (1337)	480	16	CX	0	0
(845) Naema: (21257)	390	43	CX	0	0
(293) Brasilia: (3985)	440	24	CX	3	17
(24) Themis: (981)	310	700	CX	9	50
(221) Eos: (320)	165	738	S	379	132
(10) Hygiea: (867)	290	426	CX	6	36
(283) Emma: (3369)	270	43	CX	0	0
(490) Veritas: (5592)	240	148	CX	2	9
(3556) Lixiaohua: (18477)	255	69	CX	1	0
(96) Aegle: (29579)	290	21	CX	2	0
(137) Meliboea: (1165)	270	73	CX	3	1
(1040) Klumpkea/Tirela: (18399)	290	21	CX	2	0
(778) Theobalda:(3432)	310	34	CX	0	2
(781) Kartivelia:(11911)	280	26	CX	1	0
(702) Alauda/Luthera: (11911)	420	158	CX	2	19
(31) Euphrosyne: (16712)	575	75	CX	0	3

7 CYBELE GROUP

The Cybele group, usually not considered part of the main belt, is located beyond the 2J:-1A mean motion resonance in semi-major axis and its orbital region is usually defined to lie between 3.27 and 3.70 AU in proper a and to $i < 30^\circ$. Currently, there are 1111 asteroid in the Cybele orbital region. The largest collisional family in the region is associated with (87) Sylvia, a triple asteroid (Vokrouhlický et al. 2010). The same authors investigated the orbital region of two other large binary asteroids in the region, (107) Camila and (121) Hermione, that are currently not part of any recognizable family. They concluded that, while it is possible that Yarkovsky/YORP driven mobility in the orbital region of these asteroids may have depleted possible local collisional families in timescales of 4 Byr, other mechanisms, such as resonance sweeping or other perturbing effects associated with the late Jupiter's inward migration may have been at play in the region in order to justify the current lack of dynamical groups. The AstDyS report three more families in the region of the Cybele group: Huberta, Ulla, and (2000) EK76. No halo group was found for the (2000) EK76 AstDyS cluster, that will not therefore be treated in this section. There were 128 asteroids in our multi-domain sample in this region, and we will start our analysis by investigating the Sylvia family halo.

7.1 The Sylvia family

The Sylvia family was first identified in Nesvorný et al. (2006) and was the first dynamical group found in the Cybele region. Its dynamical evolution was studied in detail in Vokrouhlický et al. (2010). In this work we identified a CX-complex halo of 13 members at a cutoff d_{md} of 395 m/s. There were no SDSS-MOC4 interlopers, and just one object (7.7% of the total) was identified as a possible albedo interloper.

7.2 The Huberta family

The Huberta family is a group reported at the AstDyS site. We identified a CX-complex halo of 4 members at a cutoff of 495 m/s. One object (25.0% of the total) was a possible SDSS-MOC4 and albedo interloper.

7.3 The Ulla family

The Ulla family is a very isolated group at relatively high inclination of $\sin(i) \simeq 0.3$ and sligthly lower than the center of the ν_6 secular resonance. It is listed as a dynamical family at the AstDys site, and we identified a small CX-complex halo of four members for cutoffs larger than 220 m/s. No interlopers were identified in this halo.

7.4 Cybele group: an overview

We summarize our results for the Cybele group in Table 5, that has the same format as similar tables used for the inner, central, and outer main belt.

Fig. 13, panel A, displays an $(a, sin(i))$ projection of asteroids in our multi-variate sample in the outer main belt, with the same symbols used for analogous figure for the inner, central, and outer main belt. Here, however, blue lines

Table 5. Asteroid families halos in the Cybele group.

First halo member	d_{md} cutoff value $[m/s]$	Number of members	Spectral likely interlopers	Number of SDSS-MOC4 Complex	Number of p_V likely interlopers
(87) Sylvia: (18959)	395	13	CX	0	1
(260) Huberta: (260)	495	4	CX	0	1
(909) Ulla: (85036)	>220	4	CX	0	0

show the location of the main linear secular resonances, using the second order and fourth-degree secular perturbation theory of Milani and Knežević (1994) to compute the proper frequencies g and s for the grid of (a, e) and $(a, \sin(i))$ values shown in Fig. 13, panel A, and the values of angles and eccentricity of (87) Sylvia, the asteroid associated with the largest family in the region (Vokrouhlický et al. 2010). We also display the location of the z_1 secular resonance as a red line, since this resonance is important in the dynamical evolution of the Sylvia group. In panel B of the same figure we display a density map of the outer main belt, according to the approach described in Carruba and Michtchenko (2009). To quantitatively determine the local density of asteroids, we computed the log_{10} of the number of all asteroids with proper elements per unit square in a 67 by 67 grid in a (starting at $a = 3.27$ AU, with a step of 0.015 AU) and $sin(i)$ (starting at 0, with a step of 0.015). The other symbols are the same as in Fig. 4, panel B.

To study how the family halos found in this work are related to the local taxonomy, we also plotted in Fig. 14 a projection in the $(a^*, i - z)$ plane of all asteroids in our multi-domain sample (panel A), and an $(a, sin(i))$ projection of the same asteroids, (panel B). The majority of asteroids in the Cybele region belong to the CX-complex, but there is a sizable minority of S-complex bodies. This is confirmed by WISE p_V geometrical albedo data, a histogram of which is presented in Fig. 15, panel A. Fig. 15, panel B, displays an $(a, sin(i))$ projection of the same asteroids, with the same color code used in similar figures for the inner, central, and outer main belt. The vast majority of asteroids in the Cybele region are dark objects, typical of CX-complex taxonomy. Overall, the predominance of dark, CX-complex asteroids in the Cybele group, confirms the taxonomical analysis performed by Vokrouhlický et al. (2010). The last region to be analyzed in this work will be that of the Hungaria asteroid family.

8 THE HUNGARIA REGION

The Hungaria region is located at the inner edge of the asteroid main belt (at semi-major axis $a < 2$ AU), and it is located at high inclinations and low to moderate eccentricities. The limitations in eccentricity allow for a perihelion large enough to avoid strong interactions with Mars, even considering secular changes in the Mars eccentricity. (Milani et al. 2010). The ν_3 and ν_5 secular resonances fix the dynamical limits of the Hungaria region in inclination. Only one family has been so far positively identified in the Hungaria orbital region, the namesake (434) Hungaria group by Milani et al. (2010). Other authors (Cañada-Assandri et al. 2013) pointed out that the highly inclined Hungaria population is dominated by S-type objects, and fairly distinguished from the C-complex population observed in the Hungaria dynamical family. But no family in proper elements domain has yet been observed in this highly inclined region. We identified only 37 objects in our multi-domain sample, with reasonable errors, and we will start our analysis of the Hungaria region by studying the Hungaria family halo.

8.1 The Hungaria family

The most recent identification of the Hungaria family was obtained by Milani et al. (2010), that also found no evidence for other possible dynamical groups in the region (but identified possible sub-structures inside the Hungaria family). Here we identified a 2 CX-complex halo at a cutoff of 590 m/s. One object, 50% of the total, was however more compatible with S-complex taxonomy and could therefore be a possible interlopers. All asteroids in the halo had $p_V > 0.1$, that is usually incompatible with a CX-complex taxonomy, but that seems typical of Hungaria objects, as discussed by Warner et al. (2009).

8.2 The highly inclined Hungaria population

No family has been currently identified in the highly inclined ($\sin(i) > 0.4$) Hungaria region in the domain of proper elements. Cañada-Assandri et al. (2013) pointed out that the highly inclined Hungaria region is dominated by S-complex objects, and taxonomically fairly different than the members of the CX-complex Hungaria group. While no family is yet identifiable in the proper element domain in this region, we checked for the presence of a halo, possibly associated with hypothetical local frequency families. We identified a S-complex halo of 7 members at a cutoff $d_{md} = 655$ m/s, around (2049) Grietje. One object, 14.3% of the total, is a possible SDSS-MOC4 interlopers, and there were no albedo interlopers.

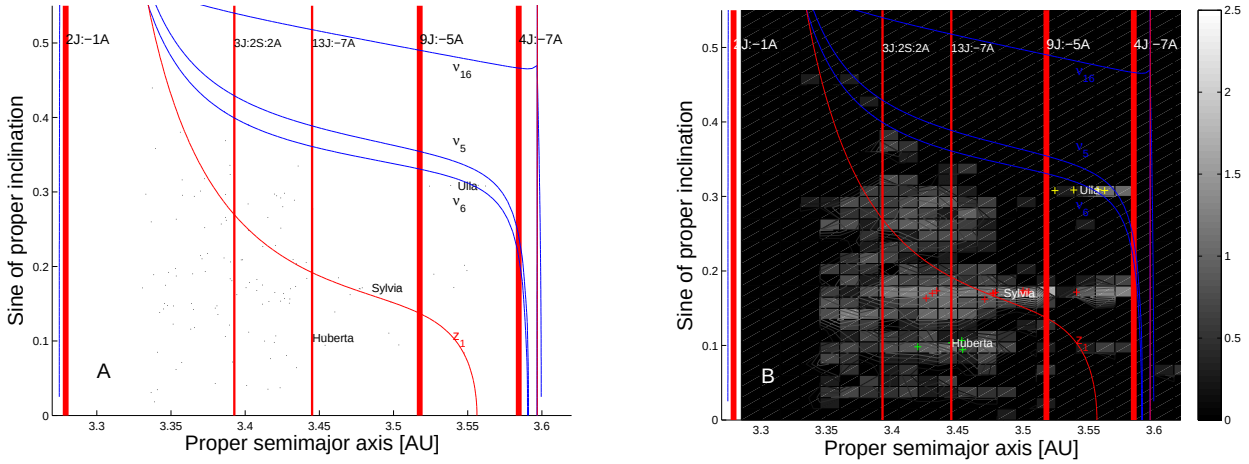

Figure 13. Panel A: An $(a, sin(i))$ projection of Cybele-group asteroids in our multi-variate sample. Panel B: contour plot of the number density of asteroids in the proper element sample. Superimposed, we display the orbital location of asteroids of families in the CX-complex (plus signs).

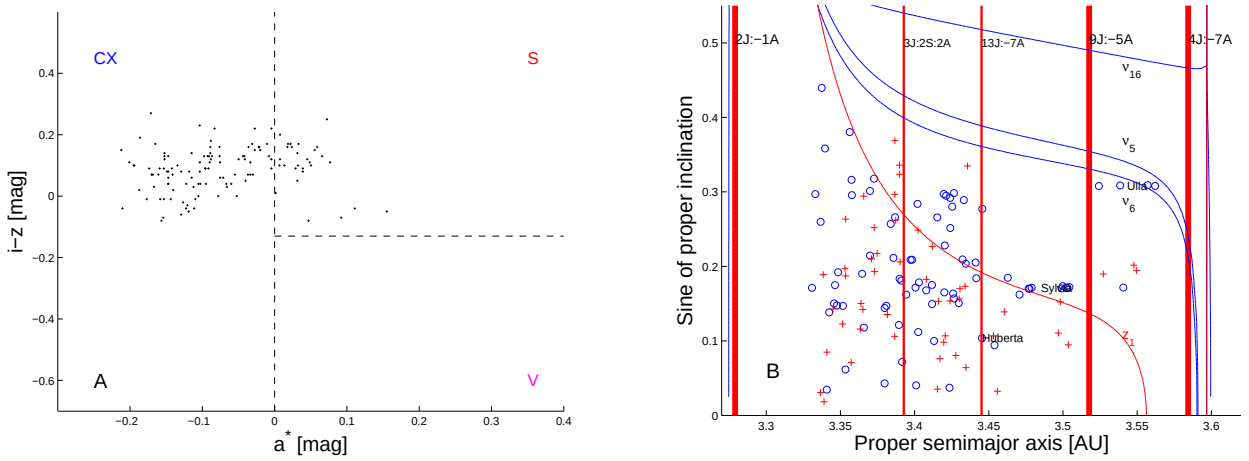

Figure 14. Panel A: an $(a^*, i-z)$ projection of Cybele-group asteroids in our multi-domain sample. Panel B: an $(a, sin(i))$ projection of the same asteroids, where objects in the CX complex are shown as blue circles, and asteroids in the S-complex are identified as red plus signs.

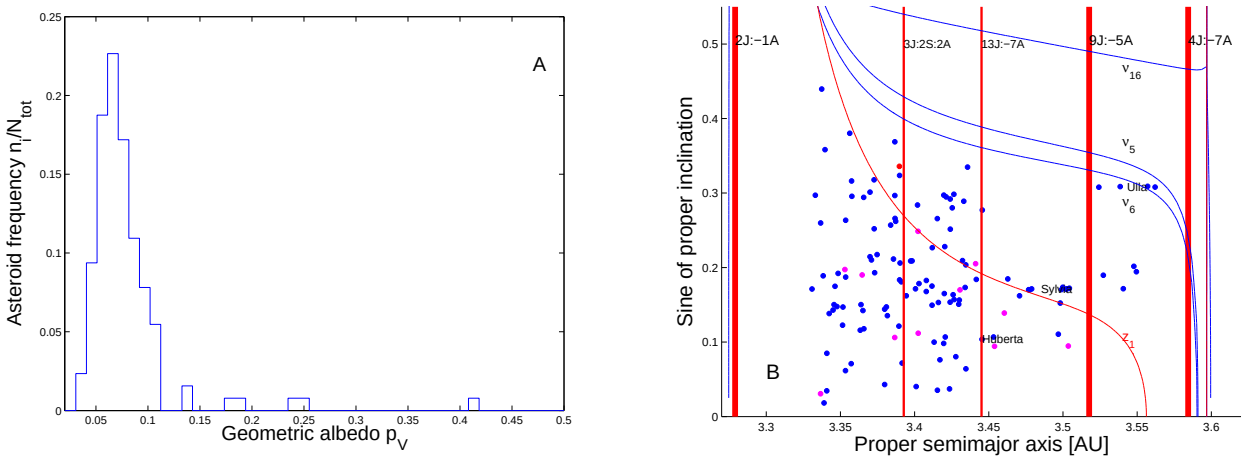

Figure 15. Panel A: a histogram of number frequency values n_i/N_{Tot} as a function of geometric albedo p_V for Cybele-group asteroids in our multi-domain sample. Panel B: an $(a, sin(i))$ projection of the same asteroids, where blue full dots are associated with asteroids with $p_V < 0.1$, red full dots display asteroids with $0.1 < p_V < 0.3$, and magenta full dots show asteroids with $p_V > 0.3$.

Table 6. Asteroid families halos in the Hungaria region.

First halo member	d_{md} cutoff value $[m/s]$	Number of members	Spectral likely interlopers	Number of SDSS-MOC4 Complex	Number of p_V likely interlopers
(434) Hungaria: (5968)	590	2	CX	1	2
(2049) Grietje: (3043)	655	7	S	1	0

8.3 The Hungaria region: an overview

We summarize our results for the Hungaria region in Table 6, that has the same format as similar tables used for the inner, central, outer main belt, and Cybele group.

Fig. 16, panel A, displays an $(a, sin(i))$ projection of asteroids in our multi-variate sample in the outer main belt, with the same symbols used for analogous figures in the inner, central, and outer main belt, and the Cybele region. Here, however, blue lines show the location of the ν_5 linear secular resonances, using the second order and fourth-degree secular perturbation theory of Milani and Knežević (1994) to compute the proper frequencies g and s for the grid of (a, e) and $(a, \sin(i))$ values shown in Fig. 13, panel A, and the values of angles and eccentricity of (434) Hungaria, the asteroid associated with the largest family in the region. We also display the location of the ν_4, ν_3 (blue lines), and ν_{14} (red line) secular resonances, since this resonance are important in setting dynamical boundaries in the region; The orbital position in the $(a, \sin(i))$ plane of the first numbered asteroid in all the Hungaria groups is also identified in Fig. 13, panel A. In panel B of the same figure we display a density map of the outer main belt, according to the approach described in Carruba and Michtchenko (2009). To quantitatively determine the local density of asteroids, we computed the log_{10} of the number of all asteroids with proper elements per unit square in a 15 by 24 grid in a (starting at $a = 1.8$ AU, with a step of 0.015 AU) and $sin(i)$ (starting at 0.25, with a step of 0.015). The other symbols are the same as in Fig. 4, panel B.

To study how the family halos found in this work are related to the local taxonomy, we also plotted in Fig. 17 a projection in the $(a^*, i-z)$ plane of all asteroids in our multi-domain sample (panel A), and an $(a, sin(i))$ projection of the same asteroids, (panel B). The majority of asteroids in the Hungaria region in our sample belong to the S-complex, but there is a sizeable minority of CX-complex bodies.

The analysis of WISE p_V geometrical albedo data, a histogram of which is presented in Fig. 18, panel A, show some peculiarities. Fig. 18, panel B, displays an $(a, sin(i))$ projection of the same asteroids, with the same color code used in similar figures for the inner, central, and outer main belt. The vast majority of asteroids in the Hungaria region and the Hungaria family are very bright objects, typical of S-complex taxonomy. The fact that many asteroids in the Hungaria family show high albedo and CX-taxonomy remains yet to be explained.

9 CONCLUSIONS

In this work we:

- Introduced a new method to obtain asteroid families and asteroid family halos based on a distance metric in a multi-domain composed of proper elements, SDSS-MOC4 $(a^*, i-z)$ colors, and WISE geometrical albedo p_V.
- Compared this new distance metric with other distance metrics in domain of proper elements, proper elements and SDSS-MOC4 colors, and proper elements and geometric albedo. The method is at best a factor of two more efficient in eliminating interlopers than other methods, and at worst it provides comparable results to groups found in domains of proper elements and SDSS-MOC4 colors only.
- Applied this method to all the major known families in the asteroids' main belt, and in the Cybele and Hungaria orbital regions. Overall, we identified sixty-two asteroid families halos, of which seven were in the inner main belt, thirty-one in the central main belt, nineteen in the outer main belt, three in the Cybele group, and two in the Hungaria region. We confirm the taxonomical analysis performed by Mothé-Diniz et al. (2005), Nesvorný et al. (2006), Carruba (2009a,b), (2010a,b) and other authors, with some small discrepancies for a few minor families in the central main belt.

Overall, apart from a few problematic cases such as the Eos family, our method appears to provide robust results in terms of asteroid family identification and in efficiency in eliminating interlopers from the clusters. While the sample of objects with data in all three domains is still limited, we believe that such an approach may be certainly more reliable than traditional HCM in identifying possible collisional groups. The possible future increase in the number of asteroids for which data in all three domains will be available, for instance because of the GAIA mission, may provide in the future data-bases for asteroid family identification much larger than the one used in this work.

Many other applications of this new approach are possible with current data-bases. An analysis of asteroid families in domains of proper frequencies such as $(n, g, g+s)$ (Carruba and Michtchenko 2007, 2009), where g is the precession frequency of the longitude of pericenter, and s the precession frequency of the longitude of the node, SDSS-MOC4 colors, and WISE albedo, may provide useful insights on the secular evolution of asteroid families. Many exciting years of discoveries are still open, in our opinion, in the field of asteroid dynamics.

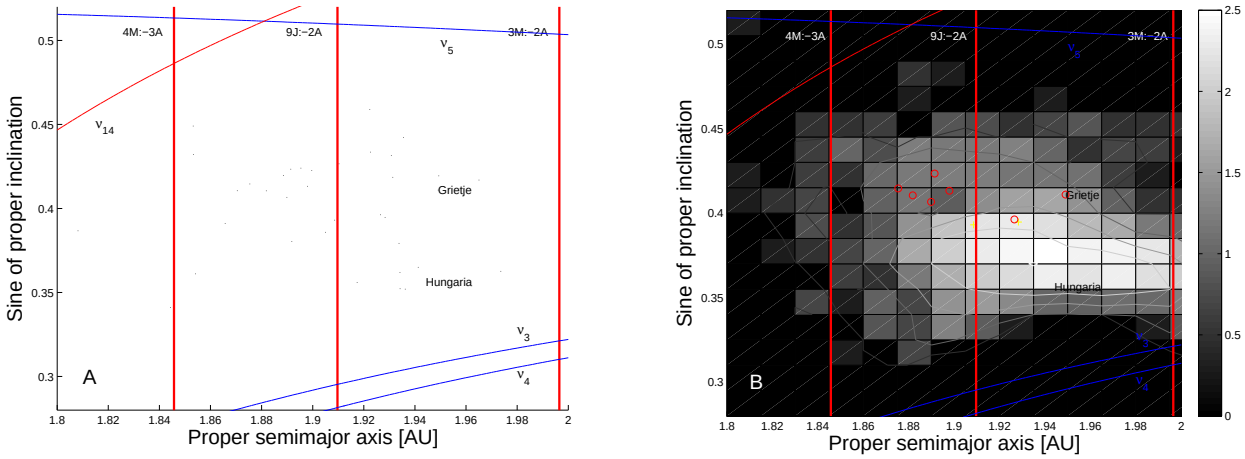

Figure 16. Panel A: An $(a, sin(i))$ projection of Hungaria-region asteroids in our multi-variate sample. Panel B: contour plot of the number density of asteroids in the proper element sample. Superimposed, we display the orbital location of asteroids of families in the CX-complex (plus signs) and S-complex (circles).

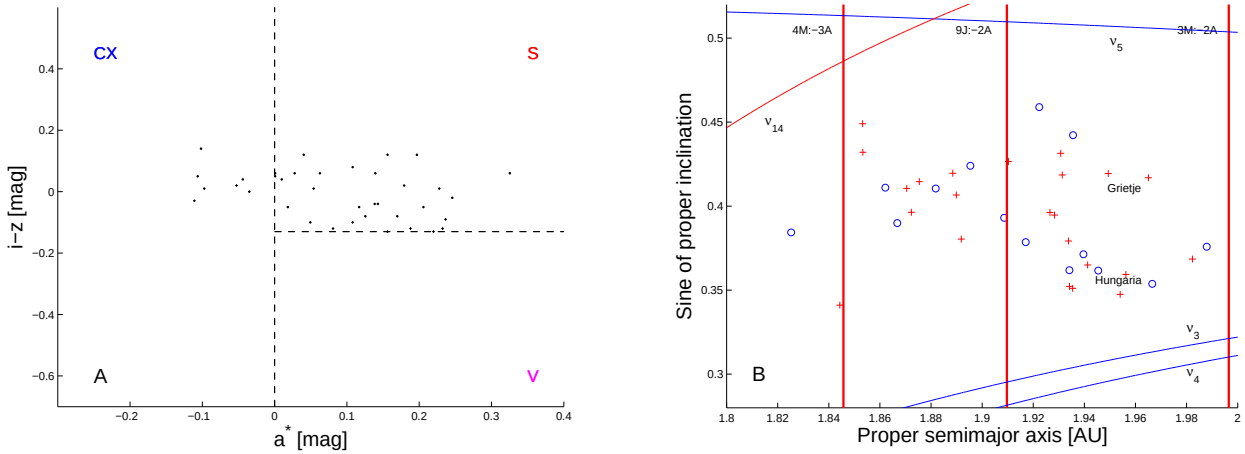

Figure 17. Panel A: an $(a^*, i-z)$ projection of Hungaria-region asteroids in the in our multi-domain sample. Panel B: an $(a, sin(i))$ projection of the same asteroids, where objects in the CX complex are shown as blue circles, and asteroids in the S-complex are identified as red plus signs.

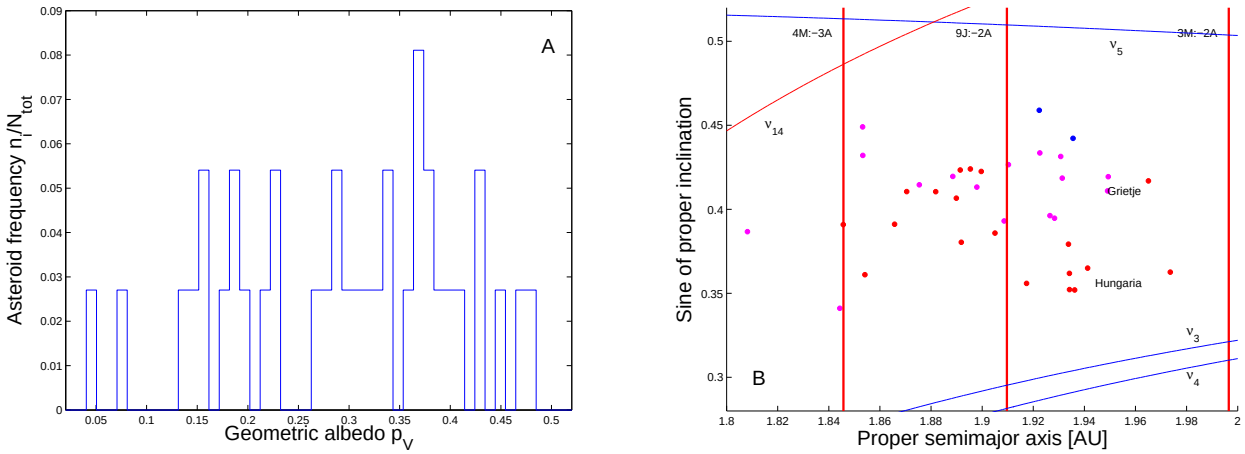

Figure 18. Panel A: a histogram of number frequency values n_i/N_{Tot} as a function of geometric albedo p_V for Hungaria-region asteroids in our multi-domain sample. Panel B: an $(a, sin(i))$ projection of the same asteroids, where blue full dots are associated with asteroids with $p_V < 0.1$, red full dots display asteroids with $0.1 < p_V < 0.3$, and magenta full dots show asteroids with $p_V > 0.3$.

ACKNOWLEDGMENTS

We are grateful to the reviewer of this article, Ricardo Gil-Hutton, for suggestions and comments that significantly increased the quality of this paper. We would also like to thank the São Paulo State Science Foundation (FAPESP) that supported this work via the grant 11/19863-3, and the Brazilian National Research Council (CNPq, grant 305453/2011-4). This publication makes use of data products from the Wide-field Infrared Survey Explorer, which is a joint project of the University of California, Los Angeles, and the Jet Propulsion Laboratory/California Institute of Technology, funded by the National Aeronautics and Space Administration. This publication also makes use of data products from NEOWISE, which is a project of the Jet Propulsion Laboratory/California Institute of Technology, funded by the Planetary Science Division of the National Aeronautics and Space Administration. Our data on asteroid families identification will be available at this site: http://www.feg.unesp.br/∼vcarruba/Halos.html

REFERENCES

Bendjoya, P., Zappalà, V. 2002. Asteroids III, Univ. of Arizona Press, Tucson, 613.
Bottke, W. F., Vokrouhlický, D., Rubincam, D. P., Brož, M. 2002, Asteroids III, Univ. of Arizona Press, Tucson, 395.
Brož, M., Morbidelli, A., 2013, Icarus, 223, 844.
Bus, J. S., 1999, Compositional structure in the asteroid belt: results of a spectroscopic survey. PhD thesis. MIT.
Bus, J. S., Binzel, R. P. 2002a, Icarus 158, 106.
Bus, J. S., Binzel, R. P. 2002b, Icarus 158, 146.
Cañada-Assandri, M., Ribeiro, A. O., Gil-Hutton, R., 2013, A&A, submitted.
Carruba, V., Burns, J., A., Bottke, W., Nesvornỳ, D. 2003, Icarus, 162, 308.
Carruba, V., Michtchenko, T., A., Roig, F., Ferraz-Mello, S., Nesvorný, D., 2005, A&A 441, 819.
Carruba, V., Michtchenko, T., A., 2007, A&A, 475, 1145.
Carruba, V., Michtchenko, T., Lazzaro, D. 2007, A&A, 473, 967.
Carruba, V., MNRAS, 2009a, 395, 358.
Carruba, V., MNRAS, 2009b, 398, 1512.
Carruba, V., Michtchenko, T., 2009, A&A, 493, 267.
Carruba, V., MNRAS, 2010a, 403, 1834.
Carruba, V., MNRAS, 2010b, 408, 580.
Carruba, V., Morbidelli, A., 2011, MNRAS, 412, 2040.
Carruba V., Huaman, M., Domingos, R. C., Roig, F., 2013, A&A, 550, A85.
Carruba V., 2013, MNRAS, 431, 3557.
Gil-Hutton, R., 2006, Icarus, 183, 93.
Hergenrother, C. W., Larson, S. M., Spahr, T. B. (1996), Bull. Am. Astron. Soc. 28, 1097.
Ivezić, Ž, and 34 co-authors, 2002, AJ, 122, 2749.
Knežević, Z., Milani, A., 2003, A&A, 403, 1165.
Machuca, J. F., Carruba, V., 2011, MNRAS, 420, 1779.
Mainzer, A. K., and 35 co-authors, 2011, ApJ 731, 53.
Masiero, J. R., and 17 co-authors, 2011, ApJ 741, 68.
Milani, A., Knežević, Z., 1994, Icarus, 107, 219.
Milani, A., Farinella, P., 1994, Nature, 370, 40.
Milani, A., Knezević., Z., Novaković, B., Cellino, A., 2010, Icarus, 207, 769.
Michtchenko T. A., Lazzaro D., Carvano J. M., Ferraz-Mello S. 2010, MNRAS 401, 2499.
Migliorini, F., Zappalà, V., Vio, R., Cellino, A., 1995, Icarus, 118, 271.
Mothé-Diniz, T., Roig, F. Carvano, J. M. 2005, Icarus, 174, 54.
Nesvorný, D., Bottke, W. F., Dones, L., Levison, H. F. 2002, Nature, 417, 720.
Nesvorný, D., Jedicke, R., Whiteley, R., Ivezić, Ž. 2005, Icarus, 173, 132.
Nesvorný, D., Bottke, W. F., Vokrouhlický, D., Morbidelli, A., Jedicke, R., 2006, proceedings of IAU symposium, Asteroids, Comets, Meteors, 229, Eds. Lazzaro, D., Ferraz-Mello, S., Fernandes, J. A., 289.
Nesvorný, D., F. Roig, B. Gladman, D. Lazzaro, V. Carruba, and T. Moth-Diniz 2008. Icarus, 183, 85.
Nesvorny, D., Nesvorny HCM Asteroid Families V2.0. EAR-A-VARGBDET-5-NESVORNYFAM-V2.0. NASA Planetary Data System, 2012.
Novaković, B., Tsiganis, K., Knežević, Z. 2010, Celest. Mech. Dyn. Astr. 107, 35.
Novaković, B., Cellino, A., Knežević, Z. 2011, Icarus, 216, 69.
Parker, A., Ivezić, Ž., Jurić, M., Lupton, R., Sekora, M. D., Kowalski, A., 2008, Icarus, 198, 138.
Roig F., Gil-Hutton R., 2006, Icarus, 183, 411.
Russel, C. T., and 27 co-authors, 2012, Science, 336, 684.
Tedesco, E. F., Noah, P. V., Noah, M., Price, S. D. 2002, AJ, 123, 1056
Tanga, P., Cellino, A., Michel, P., Zappal, V., Paolicchi, P., dellOro, A., 1999. Icarus, 141, 65.
Tholen, D. J., 1989, Asteroid Taxonomic Classifications, in Binzel R. P., Gehrels, T., Matthews, M. S. (eds), University of Arizona Press, Tucson, 298.
Vokrouhlický, D., Brož, M., Bottke, W. F., Nesvorný, D., Morbidelli, A. 2006, Icarus, 183, 349.
Vokrouhlický, Nesvorný, D., Bottke, W. F., Morbidelli, A. 2010, AJ, 139, 2148.
Warner, B.D., Harris, A. W., Vokrouhlický D., Nesvorný D., Bottke, W. F. 2009, Icarus, 398, 1512.
Williams, J. G., 1992, Icarus, 96, 251.
Wright, E. L., and 38 co-authors, 2010, AJ, 140, 1868.
Zappalà, V., Cellino, A., Farinella, P., Knežević. Z., 1990, AJ, 100, 2030.
Zappalà, V., Bendjoya, Ph., Cellino, A., Farinella, P., Froeschlé, C., 1995, Icarus, 116, 291.
Zappalà, V., Cellino, A., di Martino, M., Migliorini, F., Paolicchi, P., 1997. Icarus 129, 1.

This paper has been typeset from a TEX/ LATEX file prepared by the author.

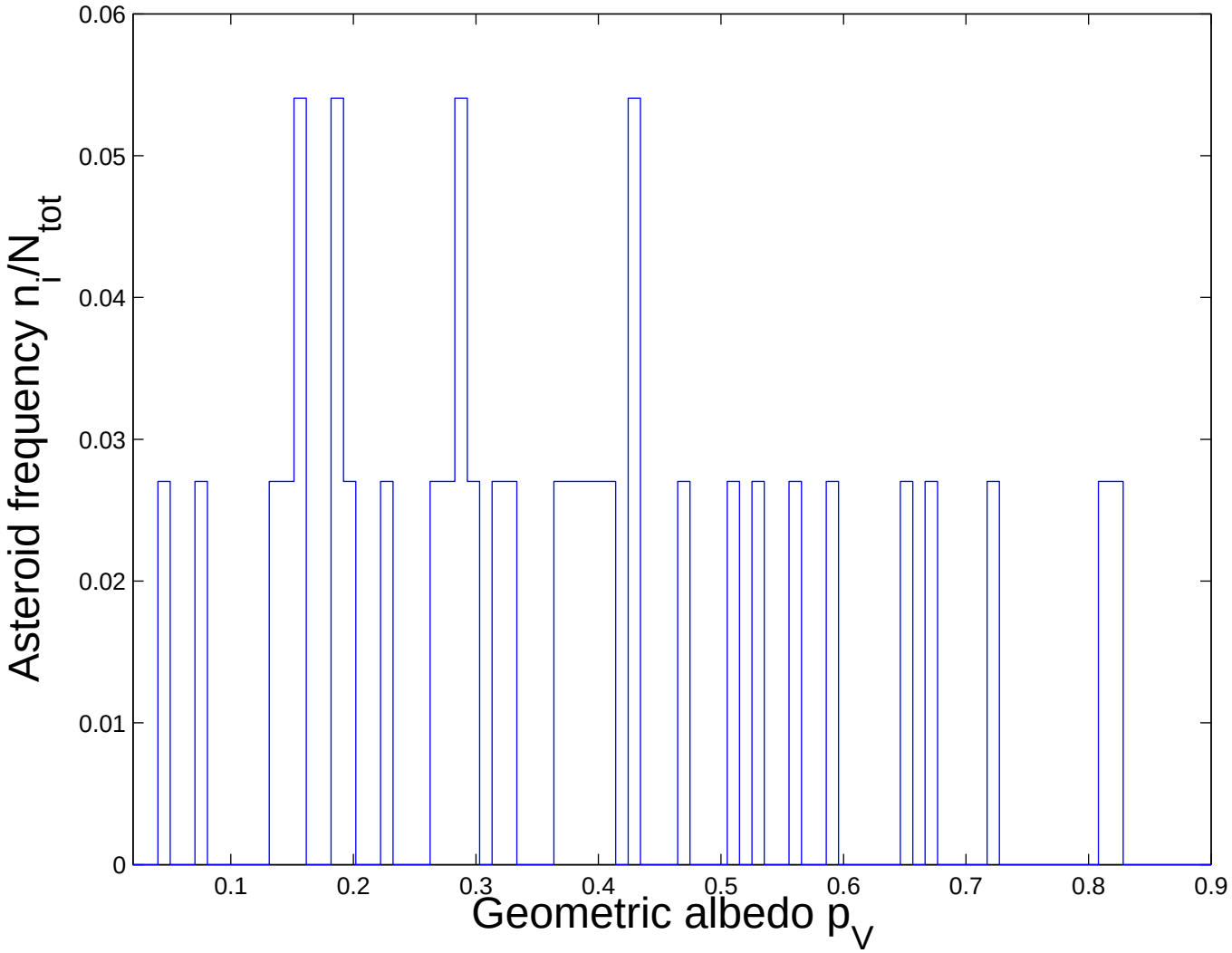
0.06
0.05
0.04
0.03
0.02
0.01
0
Asteroid frequency n_i/N_{tot}
0.1
0.2
0.3
0.4
0.5
0.6
0.7
0.8
0.9
Geometric albedo p_V

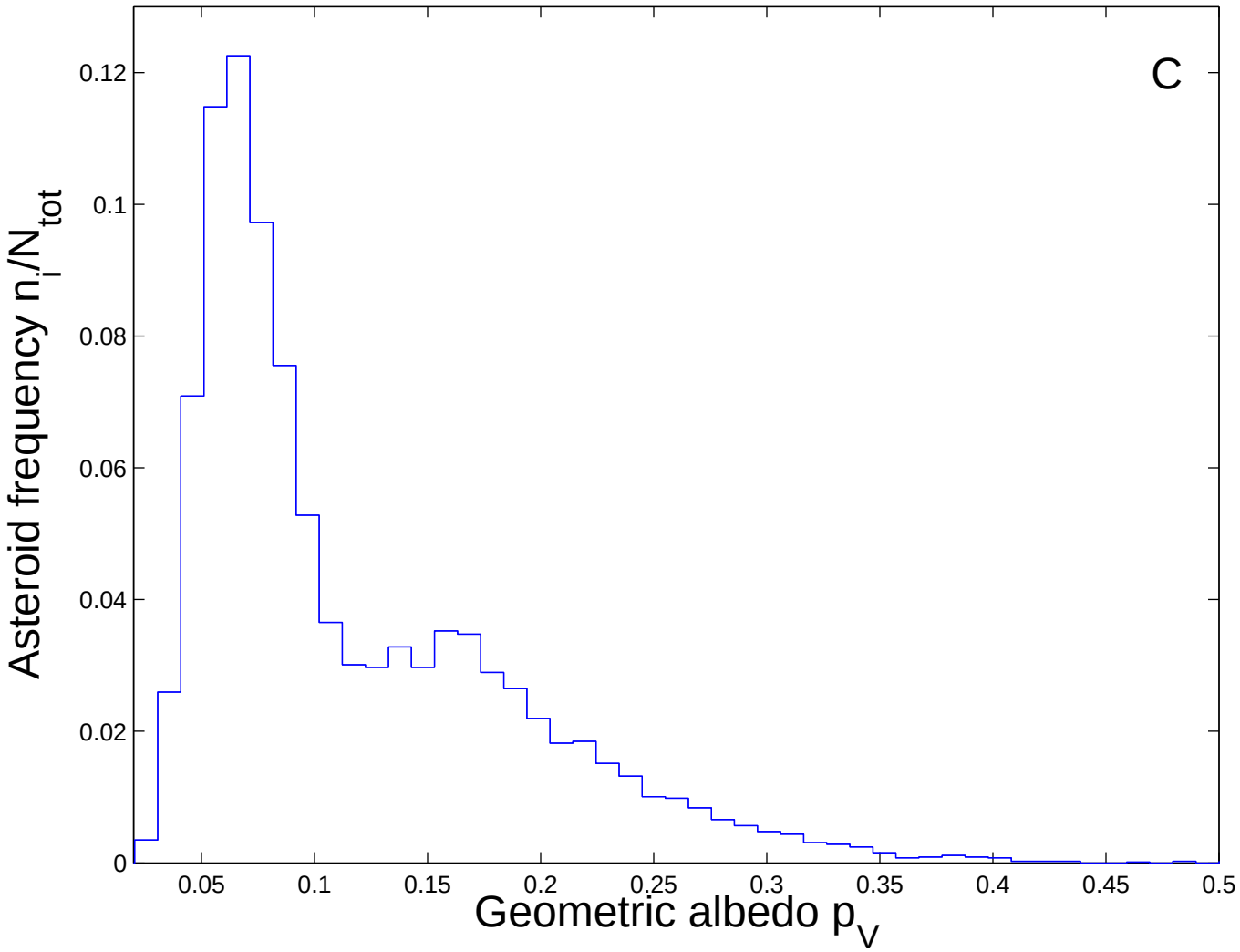
C
Asteroid frequency n_i/N_{tot}
Geometric albedo p_V
0
0.02
0.04
0.06
0.08
0.1
0.12
0.05
0.1
0.15
0.2
0.25
0.3
0.35
0.4
0.45
0.5